Dossou, Akpedje Serena, Enhancing The Solubility of Valrubicin via Albumin and TPGS Formulations. Master of Science (Biomedical Sciences), July, 2018, 64 pp., 8 tables, 34 illustrations, bibliography, 73 titles.

Human serum albumin (HSA) and D-α-tocopheryl polyethylene glycol 1000 succinate (TPGS) are versatile biocompatible materials used in drug formulation. Due to its lipophilicity, the anticancer drug valrubicin (VALSTAR) has been solubilized with Cremophor EL, a solvent known for its systemic toxicity. While valrubicin is less toxic than its widely used hydrophilic anthracycline analogues, its clinical use is currently restricted to intravesical route for bladder cancer treatment. Because preliminary studies have shown a strong affinity of valrubicin for HSA and TPGS micelles, this study was aimed to explore the potential of reduced HSA (rHSA) or TPGS as excipients for valrubicin. In an aqueous environment, valrubicin solubility was enhanced from 0.1 to 85.4% using rHSA while it was dependent upon TPGS concentration. With appropriate formulation approaches, rHSA or TPGS could serve as valrubicin transporters and could thus, enable its systemic administration and extended use beyond bladder cancer to other cancer types.

ENHANCING THE SOLUBILITY OF VALRUBICIN VIA ALBUMIN AND TPGS FORMULATIONS

THESIS

Presented to the Graduate Council of the

Graduate School of Biomedical Sciences

University of North Texas

Health Science Center at Fort Worth

in Partial Fulfillment of the Requirements

For the Degree of

MASTER OF SCIENCE

By

Akpedje Serena Dossou, B.S.

Fort Worth, Texas

July 2018

Acknowledgments

First and foremost, I would like to express my sincere gratitude to my major professor Dr. Andras Lacko for his continued support and guidance during the course of my research and the writing of this thesis. His patience, motivation and remarkable resilience inspired me to remain open-minded to new possibilities and to persevere through obstacles.

Besides my advisor, I would like to thank the rest of my thesis committee Dr. Alakananda Basu, Dr. Harlan Jones, Dr. Amalendu Ranjan and my university member Dr. Kunlin Jin for their valuable guidance and insightful comments that helped shape my project. I would also like to thank Dr. Sangram Raut, a research assistant professor in our lab. His guidance and willingness to share his expertise in fluorescence incited me to widen my research to new perspectives.

My sincere thanks go to Dr. Nirupama Sabnis and to Dr. Linda Mooberry who made our lab feel like a second “home” for me. They taught me various lab techniques mentioned in this thesis, and their contributions were thus instrumental in keeping me organized throughout my research. I thank my fellow lab mates Dr. Marlyn Panchoo, Dr. Rebecca Johnson, Bhavani Nagarajan, Ashwini Garud and Ethan Berney for their valuable feedback and for encouraging me and instilling confidence in me by sharing their personal stories in graduate study.

Last but not the least, I would like to thank my parents, my sister and my brother for supporting me emotionally and spiritually throughout this educational journey and my life in general.

TABLE OF CONTENTS

LIST OF TABLES

LIST OF ILLUSTRATIONS

CHAPTER I

INTRODUCTION

Cancer is characterized by uncontrolled cell division which ultimately results in the disruption of normal organ function. The disease evolves through a multi-stage process whereby intracellular and extracellular factors enable the normal cells to evade or switch off cell cycle surveillance mechanisms and transform into malignant cells. Usually in the late stages of malignant growth, cancer cells can acquire metastatic capability which is the most fearsome and damaging aspect of tumor progression (National Cancer Institute, 2015). Thus, cancer is a challenging disease to treat, and remains one of the leading causes of death in the United States and worldwide, second only to heart disease (WHO, 2018.). The stage and location of the disease allow the appropriate selection of treatment options ranging from non-invasive alternatives such as prescription creams- in early stages of skin tumors- to palliative care to improve quality of life, especially in the terminal stage where metastases have disseminated throughout the body and no effective curative treatment is available (American Cancer Society, 2016).

Chemotherapy and Other Cancer Treatment Options

Although novel treatment strategies have been explored for the past decade, surgery, radiation and chemotherapy remain the mainstays of cancer therapy. As the oldest treatment approach for solid tumors, surgery entails the excision of the cancerous mass (or just a portion of it in case a total removal may cause fatal damage to the affected organ) and of some of the surrounding

tissues. Best suited to treat non-metastasized and early stage cancers, surgery serves multiple purposes including prophylactic intervention, diagnosis and treatment. In radiation therapy, ionizing radiation such as beams of pi-meso, protons, neutrons, X-rays and Gamma rays are aimed at the malignant growth to cause irreversible damage to nucleic acids and biomacromolecules in cancer cells which are already unstable and possess a weak DNA repair mechanism. However, most of the time, the surrounding normal tissue is also affected by radiation. Chemotherapy uses drugs to destroy cancer cells and limit the spread of the cancerous mass (American Cancer Society, 2016).

To increase chances of success in achieving remission, surgery, radiation and chemotherapy are often used in combination. However, cancer is essentially a disease of the cell, and of these three treatment approaches, chemotherapy stands out as the one that most effectively addresses, the relevant inner mechanisms involved in carcinogenesis and metastasis of the affected cells and tissues. Drugs mainly used in chemotherapy include DNA or RNA base substituting agents (such as 5-fluorouracil or gemcitabine), DNA- damaging alkylating agents, topoisomerase inhibitors, microtubule inhibitors and hormone-regulating agents. Small molecule inhibitors of enzymes , especially kinases and specific receptors are also used with increasing frequency and offer a more targeted and personalized treatment approach (Baudino, 2015).

Whereas surgery and radiation therapy are more localized in their impact, chemotherapy drugs, especially when systemically administered, can spread throughout the body and also reach sites where there are possible metastases. In addition, for blood cancer types including leukemia and lymphoma, chemotherapy is the main form of treatment. For example, the American Cancer Society reports that for Non-Hodgkin lymphoma, chemotherapy alone is used for treatment in 58% of cases in 2013 (Fig.1).

Anthracyclines in Chemotherapy

Anthracyclines are antitumor antibiotic extracted from actinobacteria *Streptomyces peucetius*. Originally harvested for their antibacterial activity, safety studies in the early 1960's revealed that anthracyclines were more toxic to animal cells than to bacterial cells. Thus, the idea prevailed that anthracyclines could also be used against cancer cells (Bachur, 1989). Most anthracyclines exert their antineoplastic activity by intercalating between DNA bases and thus, interfering with the breaking and resealing activity of topoisomerase II. DNA replication is then disrupted, and cell cycle arrest ensues (Fig. 2). Along with taxanes which are mitotic inhibitors, anthracyclines are one of the most effective antineoplastic agents, and they include drugs such as daunorubicin, doxorubicin , idarubicin, epirubicin, amrubicin, aclarubicin , mitoxantrone, esorubicin, pirarubicin and valrubicin (Rizvi, Tariq, & Mehdi, 2018).

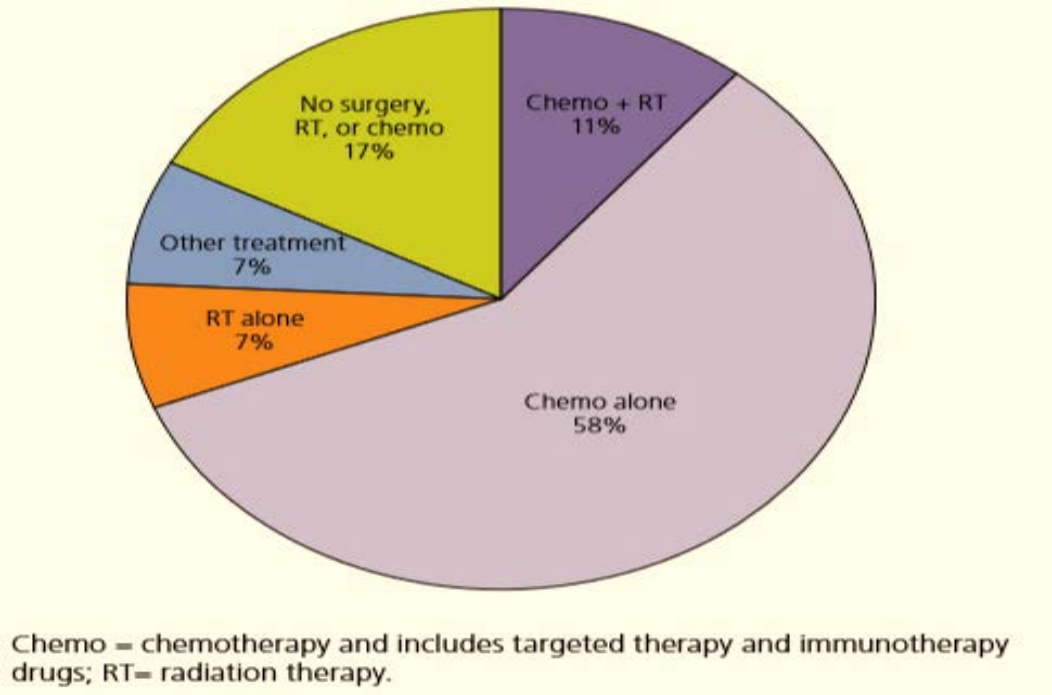

Figure 1: Treatment Application Pattern For Non-Hodgkin Lymphoma in 2013 (American Cancer Society, 2016).

Anthracyclines are used for a broad spectrum of cancers including bone cancer, breast cancer, gastric cancer, bladder cancer, liver cancer, kidney cancer, lung cancer, ovarian cancer, uterine cancer, thyroid cancer, thyomas, diverse types of leukemia and lymphomas. Although anthracyclines are known to be highly effective, they are also well known to cause cardiotoxic side effects , an aftermath of an interplay between oxidative stress, inhibition of topoisomerase II β and upregulation of death receptors elicited in cardiomyocytes (McGowan et al., 2017; Zhao & Zhang, 2017).

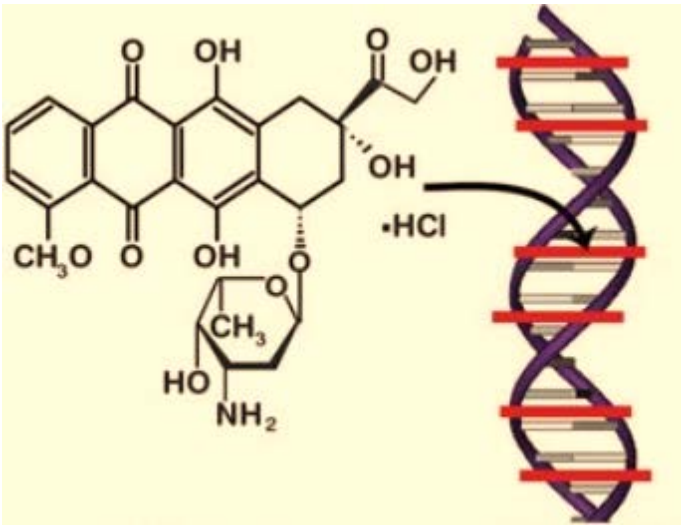

Figure 2: Doxorubicin Structure and Mechanism of Action (adapted from Gnapareddy et al., 2015). Due to its DNA-base- like structure, doxorubicin intercalates between base pairs, compromising DNA replication.

Nanomedicine: A Promising Solution for Chemotherapy's Limitations

While chemotherapy remains one the vanguards of cancer therapy, anticancer drugs like anthracyclines are generally cytotoxic for rapidly dividing cells. However, they often target normal and immune cells in addition cancer cells. These off-target effects leave cancer patients vulnerable to suffering damage to vital systems and to opportunistic infections which further

weakens them. Another cause of toxicity is the solvent with which the anticancer drugs is administered. The majority of existing and newly synthesized anticancer drugs are insoluble in water, and organic solvents/detergents which often have side effects of their own (e.g. Cremophor EL) are used in their formulation. Finally, because the accumulation at the tumor site is crucial for the effectiveness of most anticancer agents, physical biological barriers, clearance through the hepatic route or immune and renal systems are natural barriers that diminish the effectiveness of anticancer drugs (Tran, Degiovanni, Piel, & Rai, 2017).

These limitations in chemotherapy can be addressed by nanomedicine. Nanotechnology which is the study and manipulation of nanoscale objects (ideally less than 100 nm) for their application in different branches of science offers various platform tools for diagnostic, therapeutic and imaging purposes in nanomedecine. These tools include polymers, micelles, liposomes, dendrimers, proteins, metals, and they can be assembled to manufacture nanoparticles that can act as drug carriers. As drug carriers, nanoparticles are structures made (preferrably) of biocompatible materials that carry the drug either at its core or at its surface. For the whole nanoparticle structure, a diameter of more than 10 nm and less than 300 nm is recommended to avoid renal clearance and capillary occlusion in the blood circulation (Danhier, 2016).

The most powerful benefit of using nanoparticles lies in their drug delivery capabilities. First, due their small size, nanoparticles with their drug cargo can take advantage of the wider fenestration of the leaky vasculature at the tumor site to penetrate the tumor interstitium. Besides promoting drug accumulation at the tumor site, targeting moieties can be coupled to nanocarriers to increase their targeting selectivity at the site of action of the drug (Fig. 3). Secondly, when biocompaticle materials such as proteins are used as drug carriers, they eliminate the need to use organic solvents as a dissolution medium or excipient. Thus, the off-target effects resulting from

destroying normal cells can be minimized. Thirdly, most materials used as drug carriers have a long residence time in the blood and lymphatic circulation, and thus can protect their drug cargo from degradation or removal via the reticuloendothelial system (Bhushan, Khanadeev, Khlebtsov, Khlebtsov, & Gopinath, 2017).

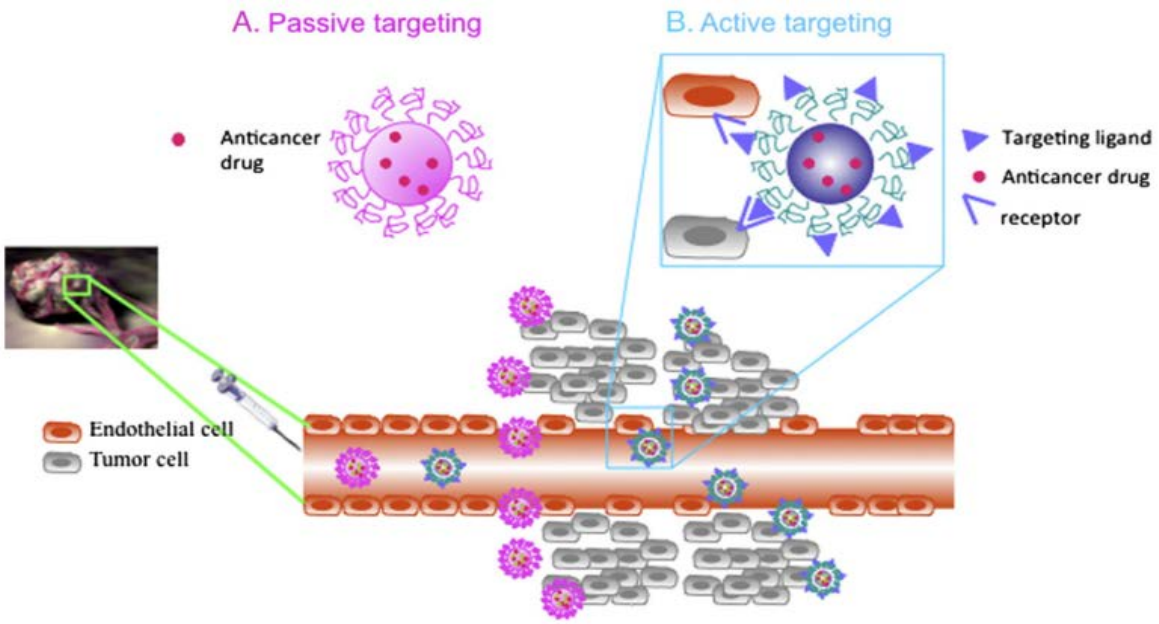

Figure 3: Pictorial Illustration of Mode of Action of Nanocarrier Systems (Bhushan et al., 2017). In passive targeting, the drug-loaded nanoparticle moves through the fenestrations of the leaky vasculature and get to the tumor cells. In active targeting, a targeting ligand is coupled to the surface of the nanocarrier system and guides it to the right cells to target.

Valrubicin: The Forgotten Anthracycline

Valrubicin (marketed as Valstar with the Cremophor EL excipient) also known as AD 32 or N-trifluoroacetyladriamycin-14-valerate (Table 1) is a derivative of the anthracycline antibiotic doxorubicin. With a molecular weight of 723.64 g/mol, valrubicin is a red -orange amorphous powder with intrinsic fluorescence properties. Currently, valrubicin is FDA approved for treating carcinoma in situ Bacillus Calmette-Guerin (CIS-BCG) resistant bladder cancer. Valrubicin

effectively disrupts DNA and RNA synthesis in cancer cells (Israel, Idriss, Koseki, & Khetarpal, 1987; Potmesil, Silber, Israel, Goldfeder, & Khetarpal, 1981). However, unlike doxorubicin which localizes in the nucleus once it enters the cell, valrubicin does not get to the nucleus; instead, valrubicin remains in the cytoplasm. Aside from indirectly inhibiting DNA synthesis, valrubicin and its metabolites such as AD41 (N-trifluoroacetyladriamycin) and AD92 (N-trifluoroacetyladriamycinol) produce oxidative stress in cancer cells which induces apoptosis

Table 1: Structure of Valrubicin and Its Metabolites (adapted from Potmesil et al., 1981). R1, R2 and R3 represent the functional group at the position indicated in the basic structure of adriamycin.

Basic structure of adriamycin derivatives	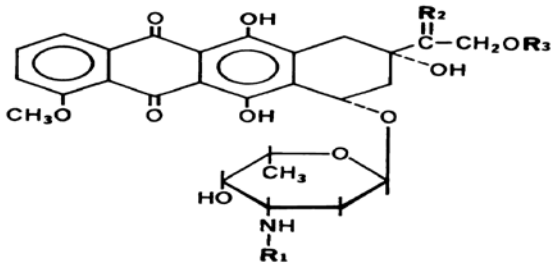		
Derivatives	**R1**	**R2**	**R3**
Valrubicin	**COCF3**	**O**	**$CO(CH_2)_3CH_3$**
AD41	**COCF3**	**O**	**H**
AD92	**COCF3**	**H, OH**	**H**

Valrubicin and Its Anthracycline Analogues

While most anthracyclines are known for their cardiotoxicity as a collateral damage, valrubicin displays much less toxicity (Table 2) towards cardiomyocytes and other normal cells and higher antitumor activity than its anthracycline analogues in early comparative studies for in

vitro and murine tumor models (Ganapathi & Israel, 1981; Israel, Modest, & Frei, 1975). In addition, in *in vitro* studies with hematopoietic stem cells and chick embryos, doxorubicin was shown to produce more toxic effects than valrubicin and a similar toxicity pattern was reported while assessing anthracycline-related cardiomyopathy in rabbits (Onrust & Lamb, 1999).

Although the reason for the reduced toxicity associated with valrubicin is still not fully understood, early studies in human lymphoblastic leukemia cells have shown that valrubicin and its cellular metabolites do not bind to DNA as doxorubicin does but, they do induced DNA–protein cross-links and protein associated DNA breaks (Potmesil et al., 1981). Rosada et al showed that in keratinocytes, AD41 (N-trifluoroacetyladriamycin) which is a metabolite of valrubicin, is evenly distributed throughout the cell (Fig. 4) and along with valrubicin, generates reactive oxygen species (Štěrba et al., 2013).

Table 2: Early Comparative Studies on Antitumor Activity and Toxicity of Anthracyclines (adapted from Israel et al., 1975). Here, valrubicin, daunorubicin and doxorubicin were administered intraperitoneally to treat male mice inoculated with highly aggressive leukemic cells line (P388 and L1210). The high optimal dose of valrubicin and the associated number of survivors attest of the beneficial reduced toxicity. N/A (not applicable).

Anthracycline Drug	Optimal Dose (mg/Kg)	Percent increase in median life span	Survivors	
			30 –day	60- day
Daunorubicin	**2.0**	**+ 91**	**0/6**	**N/A**
Doxorubicin	**4.0**	**+ 132**	**0/6**	**N/A**
Valrubicin	**40.0**	**+ 439**	**4/5**	**3/5**

Despite their cardiotoxic side effects, anthracycline analogues of valrubicin offer therapeutic application for a variety of cancer types. For instance, doxorubicin can be used for treating several solid tumors and different forms of leukemia. Such versatility is due to the relative hydrophilicity of doxorubicin (octanol to water partition coefficient Log kow = 1.27, PubChem). Hence, Doxorubicin can easily dissolve in normal saline and thus can be systemically administered. In contrast, valrubicin is practically insoluble in water (log kow = 5.06, PubChem) which is why valrubicin is only applied clinically in a non-aqueous solution at the concentration of 40mg/mL in 50% polyoxyl castor oil (Cremophor EL) /50% dehydrated alcohol (Endo Pharmaceuticals, 2011). Such formulation restricts its administration to the intravesical route due to the toxicity associated with the solubilizing agent, Cremophor EL.

Cremophor EL

Cremophor EL is synthesized by reacting ethylene oxide with castor oil, and it is often used as a vehicle for poorly water- soluble drugs. In cancer chemotherapy, Cremophor EL was the main solvent used for the intravenously administered mitotic inhibitors paclitaxel and docetaxel. In the late 1990's, the common anaphylactoid hypersensitivity reactions and exacerbated hematotoxic side effects reported for drugs formulated with Cremophor EL prompted several studies investigating the effects of cremophor on the immune system (Weiss et al., 1990). Using healthy subjects and cancer patients' sera, Szebeni and colleagues showed activation of the complement system, especially the production of the anaphylatoxins C3a and C5a by Cremophor EL (Szebeni, Muggia, & Alving, 1998). In their study, the 1:1 volume ratio of Cremophor EL and ethanol which was the then – solvent for paclitaxel -and still is the solvent for valrubicin marketed as Valstar - produced significantly higher levels of anaphylatoxins compared to Cremophor EL alone or ethanol alone.

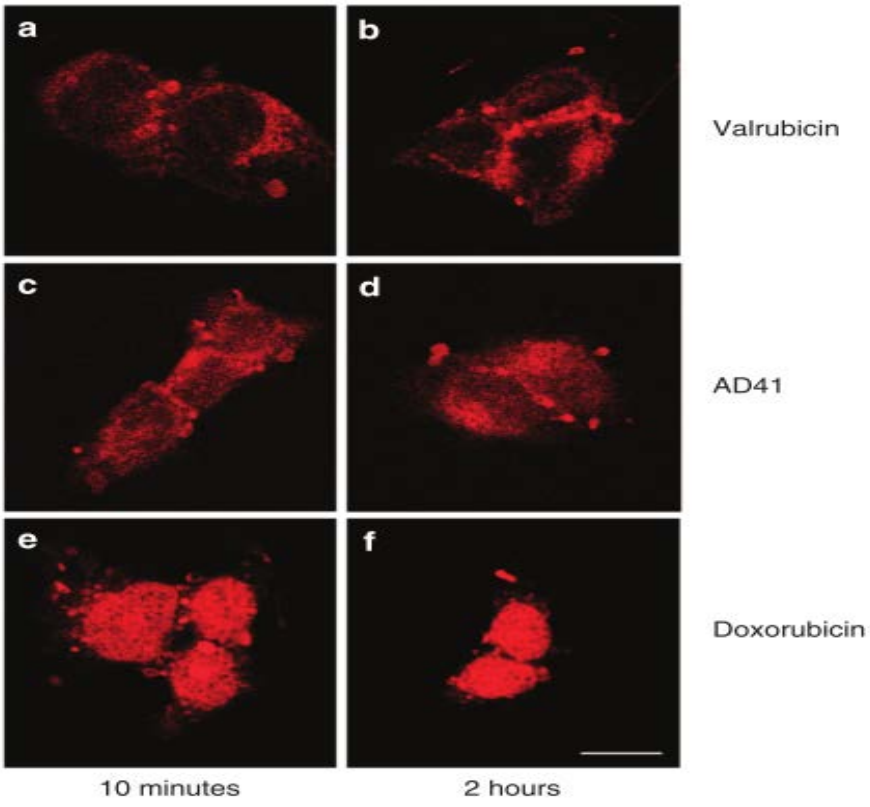

Figure 4: Cellular Localization of Valrubicin, AD41 and Doxorubicin in Keratinocytes (adapted from Rosada et al., 2010).

Cremophor EL treatment was also found to account for the systemic oxidative stress by causing oxidative damage to red blood cells in rats (Campos et al., 2014). Interestingly, preclinical studies for systemic delivery of valrubicin (Vecchi, Spreafico, Sironi, Cairo, & Garattini, 1980) and a phase I trial for gynecological malignancy (Markman et al., 1996) reported hematotoxic and hypersentivity side effects although any connection to the vehicle has yet to be investigated. As for paclitaxel, the pharmaceutical company Celgene introduced an human serum albumin-bound formulation which eliminated the need for using Cremophor EL as a solvent and highly improved tolerability, tumor accumulation and response rates of paclitaxel (Yardley, 2013).

Human Serum Albumin: Structure and Function

Synthesized by hepatocytes in the liver, human serum albumin (HSA) is a globular monomeric protein containing 585 amino acid residues with a molecular weight of 66,437 Daltons. HSA has three homologous domains in its structure: I, II and III (Fig. 5). The subdomains IIA and IIIA provide binding pockets for a variety of endogenous ligands as well as drugs. HSA is a sturdy protein that can withstand a heating up to 60^{o}C for 10 hours and remain stable in a pH range of 4 to 9 (Kratz, 2008). HSA has 35 cysteinyl groups in its structure, 34 of which form disulfide bridges, primarily responsible for its native folded structure. The remaining cysteinyl residue Cys34 offers a free thiol residue that facilitates the dimerization of the HSA molecule (Elzoghby et al., 2012). .

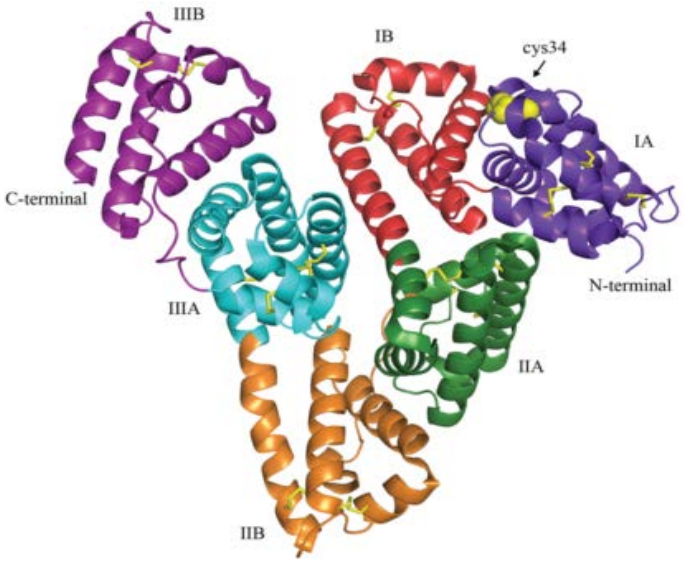

Figure 5: Structure of HSA (adapted from Larsen, Kuhlmann, Hvam, & Howard, 2016). The colors denote the different subdomains of HA and the yellow lines represent the disulfide bonds.

Being the most abundant protein in the blood (35-50 mg/mL), HSA regulates blood colloidal oncotic pressure Even so, most of the HSA produced by the liver gets out of the blood circulation

through transcytosis (vesicle mediated transport of a macromolecule across the interior of a cell from one side of the cell to the other side) or directly through fenestrations in the vascular endothelium. Thus, HSA is most of the time an extravascular protein, a characteristic which is instrumental for its natural carrier function. HSA transports a variety of endogenous ligands including hormones, vitamins, cations, bilirubin as well as fatty acids which are highly lipophilic and make these compounds available to tissues in the interstitial space. HSA returns to the blood circulation via the lymphatic system (Merlot, Kalinowski, & Richardson, 2014).

Human Serum Albumin as a Drug Vehicle

Before the emergence of HSA in the early 2000's as an efficient drug carrier, HSA alone was prescribed and administered intravenously to patients with low albumin levels, to burn victims and patients presenting with cachexia (deterioration of physical condition due to chronic illness) as a blood substitute (Kratz, 2014). Subsequently, many pharmacological studies confirmed that besides carrying endogenous materials in the blood, HSA can also reversibly bind several drugs including salicylic acid, ibuprofen, naproxen, or warfarin in its Sudlow's sites (Aarons, Grennan, & Siddiqui, 1983; Maruthamuthu & Kishore, 1987; Petitpas, Bhattacharya, Twine, East, & Curry, 2001; Merlot et al., 2014). Other pharmacological studies showed that by binding these drugs, HSA improves their bioavailability and maintains their levels in the therapeutic range as HSA has a long circulatory life (about 19 days) (Sleep, Cameron, & Evans, 2013). Being endogenously produced, HSA is non-immunogenic, biodegradable. In addition, the free thiol group on Cys34 can be used to add functional groups to HSA for targeting purposes (Elzoghby et al., 2012).

All these above-mentioned properties of HSA uncovered by several studies increased awareness of HSA as a beneficial excipient (substance that serves as solvent or vehicle for an

active substance), suitable for drug formulation. Such application of HSA has implications, particularly for drugs prescribed for chronic illness. Since these drugs are usually administered frequently, it is important that

i. the delivery vehicle (solvent or a nanocarrier system) transports effectively these drugs to their site of action
ii. none of the components of the formulation hinders the drug activity
iii. all ingredients of the formulation are safely metabolized and disposed by the body.

Hence, fulfilling all these requirements, HSA was an acceptable carrier for drugs against diabetes, hemophilia, autoimmune diseases and cancer (Table 3), especially due to the absence of HSA-related toxicity. Instead, HSA possesses anti-oxidant properties that lessen side-effects from drugs (Evans, 2002). This is markedly the case with paclitaxel for which the albumin-bound formulation has shown milder side effects than the Cremophor EL-based paclitaxel (Miele, Spinelli, Miele, Tomao, & Tomao, 2009; Yardley, 2013).

Human Serum Albumin in Anticancer Chemotherapy

As a drug carrier, HSA enters the realm of nanomedicine which uses nanoscale platforms to improve drug delivery. As previously mentioned, the benefit of using nanocarriers for anticancer drug delivery lies in their selective targeting potential, the protective shield they bestow on to their drug payload against degradation and the relatively small size of these carrier systems that permits evasion from the immune system and enhances their accumulation at the tumor site (Tran et al., 2017). As a plasma protein, HSA displays some unique features that make it suitable as a vehicle for anticancer drug delivery. First, HSA is an extravascular protein, and can easily penetrate the tumor interstitium. Two major HSA-binding proteins are responsible for the transit

of albumin from the blood circulation to the tumor interstitium: Gp60 and Secreted Protein, Acidic and Rich in Cysteine (SPARC).

Table 3: Examples of Drugs Formulated with HSA (adapted from Larsen et al., 2016, and Zhang, Sun, & Jiang, 2018)

Binding model	***Formulation Name***	***Disease***	***Drug Name***	***Developing Company***	***Clinical Status***
Nanoparticle	Abraxane	Cancer	Paclitaxel	Celgene	Marketed
	ABI-008	Cancer	Docetaxel	Celgene	Phase I/II
	ABI-009	Cancer	Rapamycin	Celgene	Phase I/II
Non-Covalent binding	Levemir	Diabetes types I and II	Insulin detemir	Novo Nordisk	Marketed
	Victoza	Diabetes type II	Glucagon-like peptide 1	Novo Nordisk	Marketed
	Ozoralizumab	Rheumatoid arthritis	Antibody	Ablynx	Phase II completed
Covalent-binding	MTX-HSA	Cancer and Autoimmune Diseases	Methotrexate	Access Pharmaceutical Inc.	Phase II
	Aldoxorubicin	Cancer	Doxorubicin	CytRx Inc.	Phase I
	CJC-1134	Diabetes Type II	Exendin 4	ConjuChem	Phase II
Gene Fusion	Eperzan	Diabetes type II	Glucagon-like peptide I	Glasso Smith Kline	Marketed
	IDELVION	Haemophilia B	Factor IX albumin fusion protein	CSL Behring GmbH	Phase III

Gp60 is an albumin receptor located on the luminal surface of vascular endothelial cells, and it mediates the transcytosis of HSA to the extravascular space. SPARC sequesters HSA in the extracellular space (Fig. 6). Although it is still at the early stage, several studies have shown that

cancer types featuring increased SPARC expression were more sensitive to albumin-bound chemotherapy than the ones with lower SPARC expression (Desai, Trieu, Damascelli, & Soon-shiong, 2009; Yardley, 2013). In addition, in non-small cell lung cancer and pancreatic cancer, sensitivity to Abraxane has been shown to depend upon the expression Caveolin-1, an indispensable protein for transcytosis (Chatterjee et al., 2017).

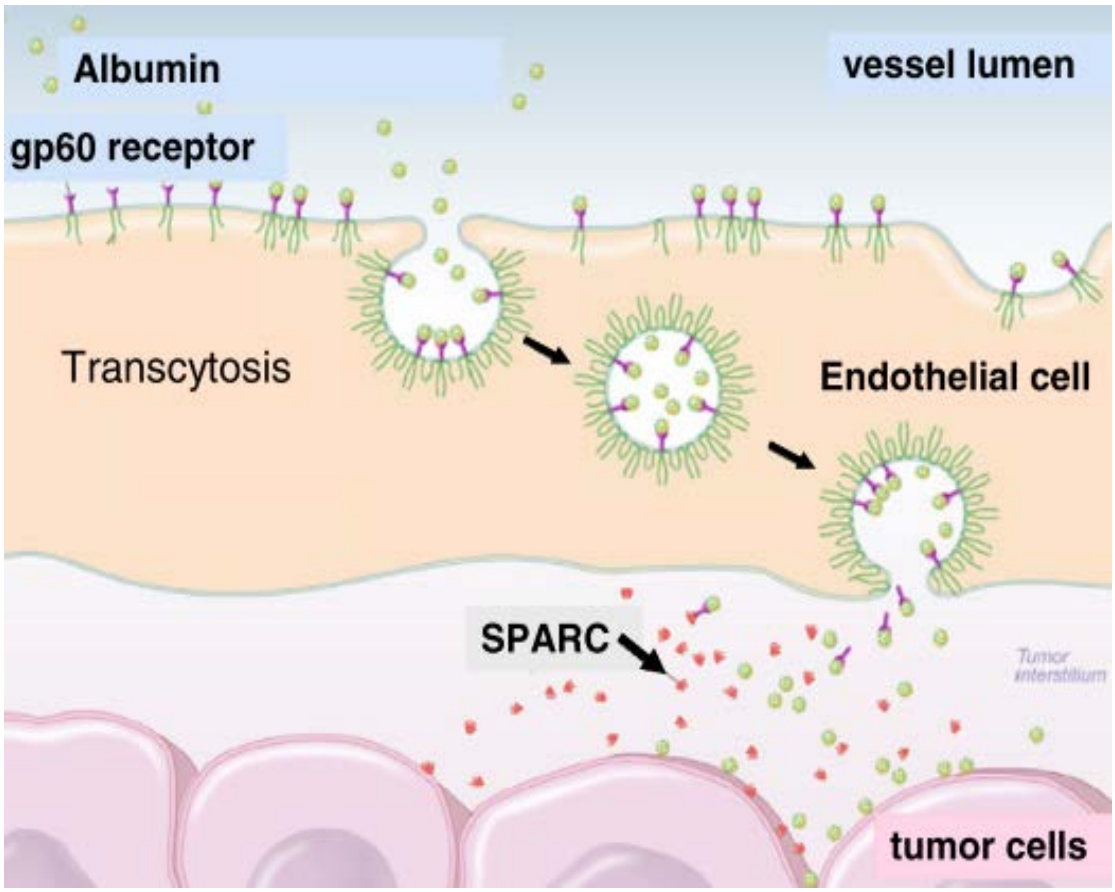

Figure 6: Transit of Human Serum Albumin from the Blood Circulation to the Tumor Site (adapted from Kudarha & Sawant, 2017). Binding of albumin molecules to the gp60 receptor on endothelial cells mediates their intracellular transport in endosomes to the tumor interstitium.

Secondly, hypoalbuminemia is often reported in patients with advanced solid tumors , and the low levels of HSA have been linked to the increase need of nutrient for the rapidly expanding

cancer tissue which avidly catabolize HSA (Merlot et al., 2014; Stehle et al., 1997). Thirdly, the leaky vasculature put together at solid tumor sites to accommodate the need for the rapid supply of oxygen and nutrient enhances the intratumoral retention of macromolecules such as HSA (Maeda, Wu, Sawa, Matsumura, & Hori, 2000). Because HSA is non-toxic, can passively and actively reach the tumor site and may be functionalized for targeting purposes, the use HSA as a carrier could benefit the delivery of anticancer drugs. For instance, regarding Abraxane, which is considered a breakthrough in using HSA in anticancer therapy, HSA effectively served as nanocarrier for paclitaxel (about 130 nm in diameter size), making the formulation suitable for intravenous injection as the risk for capillary obstruction is eliminated. HSA improved the efficacy of paclitaxel by helping overcome biological barriers such as hepatic, renal and immune clearance, and most importantly, mediated the decrease in off-target toxicity compared to the solvent-based paclitaxel (Miele et al., 2009).

TPGS: Properties and Usage in Drug Formulation

With a molecular weight of 1513 g/mol, TPGS, a nonionic surfactant, is the product of the esterification vitamin E succinate with polyethylene glycol (PEG) 1000. Thus, it has a hydrophilic head group made of PEG ($H-(O-CH2-CH2)_n-OH$, where n=22); the hydrophobic vitamin E tail is linked to the polar head by the succinate group (Fig. 7). The amphiphilic structure of TPGS promotes both its water solubility and its ability to solubilize lipophilic compounds via micelle formation (Guo, Luo, Tan, Otieno, & Zhang, 2013; Hasanuddin, Affandi, Salama, & Tripathy, 2014). Since its commercial production, TPGS has been-and still is-used as nutritional supplement for patients with vitamin E deficiency (Duhem, Danhier, & Préat, 2014; PMC isochem, 2018). Besides serving as source of vitamin E in the pharmaceutical industry, TPGS is widely used in drug formulation, especially due its micelle forming capability and its

GRAS (generally regarded as safe) status granted by the US Food and Drug Administration (FDA). Indeed, in rat studies, the quantity of TPGS that kill 50% of the test subject (LD_{50} , median lethal dose) was estimated to be more than 7g/kg for oral administration and more that 2g/kg for other administration routes (Z. Zhang, Tan, & Feng, 2012). For patients with vitamin E deficiency, TPGS can be taken orally up to 100 mg/kg/day (Yan, Von Dem Bussche, Kane, & Hurt, 2007).

Several studies have confirmed TPGS antioxidant properties, and its ability to serve as a solubilizer, an emulsifier, and permeability and absorption enhancer (Wagner, Buettner, & Burns, 1996; Yan et al., 2007). TPGS can also act as a bioavailability enhancer especially for orally administrated drugs and is recognized for its ability to overcome multidrug resistance by inhibiting the P-glycoprotein, an efflux pump which decreases the accumulation of drugs in cells (Fan et al., 2015). Amprenavir (protease inhibitor against human immunodeficiency virus), Wal-profen (Nonsteroidal anti-inflammatory drug) or Nuroprofen (Nonsteroidal anti-inflammatory drug/painkiller) are examples of marketed TPGS-based oral drug formulations that showed increase in bioavailability (Savla, Browne, Plassat, Wasan, & Wasan, 2017; Z. Zhang et al., 2012).

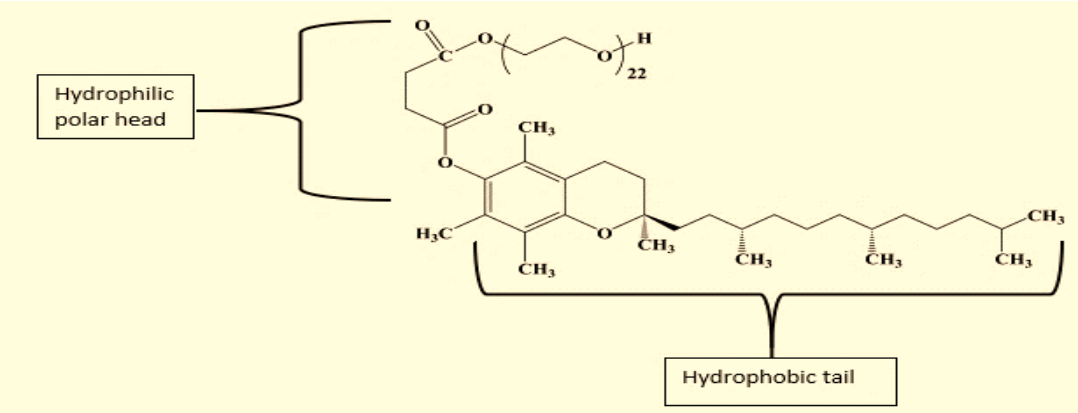

Figure 7: Chemical Structure of TPGS (adapted from Shah & Banerjee, 2011).

TPGS in Anticancer Chemotherapy

The effectiveness of anticancer drugs is dependent upon their accumulation at the site of action to a concentration that falls in the therapeutic range for a designated duration. Thus, multidrug resistance constitutes a major hurdle in treating cancer patients, especially for cases where drug-extruding efflux pumps such the P-glycoprotein are overexpressed. One of the main reasons TPGS is used as an additive in anticancer drug formulation is that TPGS can enhance drug bioavailability and absorption by inhibiting the P-glycoprotein. Because the efflux activity of the P-glycoprotein is ATP-dependent, TPGS enhances drug intracellular accumulation by causing allosteric inhibition of the ATPase activity of the efflux pump (Table 4) or by inhibiting the mitochondrial complex II in the electron transport chain, causing shortage in ATP supply (Yang, Wu, Qi, & Zhang, 2018).

Although there are no reports of TPGS-based formulation of anticancer drugs on the market or in ongoing clinical trials, there is a multitude of studies showing the benefit of TPGS as an excipient for anticancer drugs including the small size of TPGS micelles, the reduced toxicity of TPGS compared to other surfactants such as Tweens, Pluronic or Cremophor EL, and the previously discussed properties of TPGS. For instance, TPGS micelles loaded with docetaxel (a microtubule-inhibiting anticancer drug) showed significantly higher cellular uptake of docetaxel by C6 glioma cancer cells, higher cytotoxicity, and 2.54 fold penetration in rat brain tissue after 2 hours intravenous injection of the formulation compared to Taxotere, the commercial formulation of docetaxel (Muthu, Avinash Kulkarni, Liu, & Feng, 2012). Similarly, in a dosage study of a genkwanin -a insoluble flavonoid with anti-inflammatory, antioxidant and anticancer properties- formulated with TPGS against breast cancer cells, Li et al. showed enhanced cytotoxity effects compared the free genkwanin in dimethyl sulfoxide (DMSO) (Li et al., 2017)

Table 4: Applications of TPGS in Anticancer Drug Formulation (adapted from Yang et al., 2018).

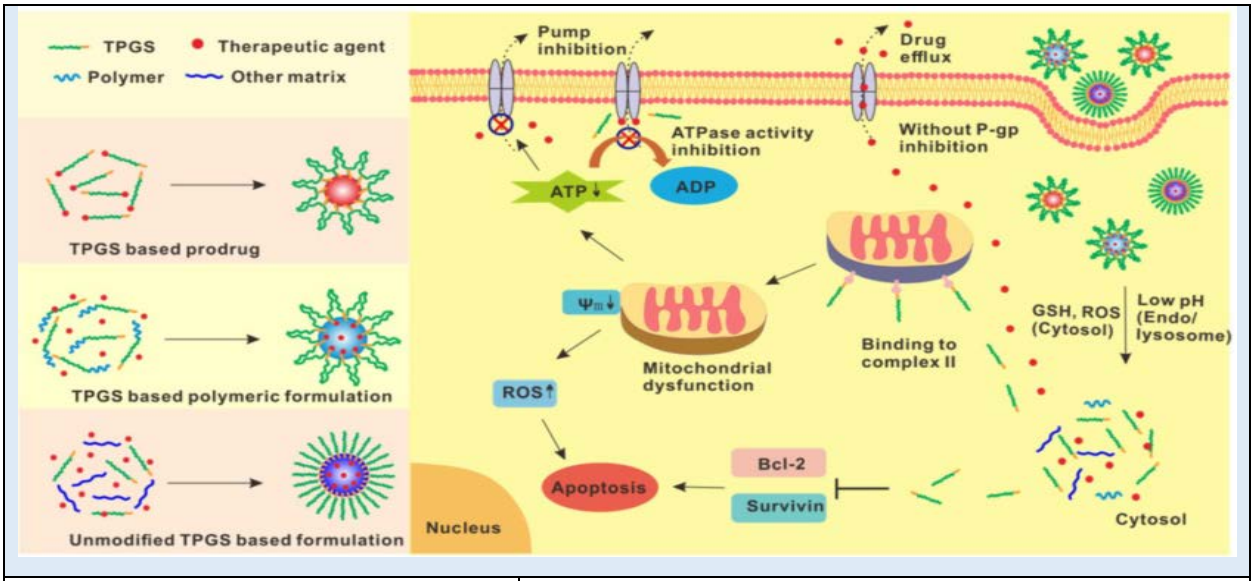

Common use of TPGS in drug formulation	Description
TPGS-based prodrugs	TPGS is covalently linked to the drug which then becomes a prodrug with low activity. Upon cellular entry, the micellar structure is hydrolyzed, and the drug regains its full pharmaceutical activity
TPGS-based polymeric formulations	TPGS is covalently linked to a biodegradable polymer or a targeting agent to form a structure with the drug at the core to improve stability, drug encapsulation efficiency, selective targeting or therapeutic effects
Unmodified TPGS-based formulations	TPGS can simply be mixed with the drug to form drug-loaded TPGS micelles or be mixed with additional surfactants to form drug loaded mixed micelles

Synergistic effects with diverse anticancer drugs have also been attributed to TPGS, especially due to its intrinsic pro-apoptotic activity. In a panel of breast cancer cell lines, Neophytou et al. reported a negative regulation of cell survival pathways upon TPGS treatment.

They showed a downregulation of phosphorylation of protein kinase B (also known as Akt) at its activating phosphorylation sites Ser^{473} and Thr^{308}, a downregulation of the antiapoptotic proteins survivin and Bcl2 as well as an upregulation of cyclin-dependent kinase inhibitors p27Kip1 and p21 (Neophytou, Constantinou, Papageorgis, & Constantinou, 2014).

Project Hypothesis and Specific Aims

During attempts to identify endogenous agents to serve as delivery vehicles for valrubicin, preliminary data from incubation experiments of valrubicin in selected human plasma components such as low-density lipoproteins (LDL), high-density lipoproteins (HDL) and HSA suggests preferential binding of valrubicin to HSA (Fig. 8). However, HSA (45mg/mL, aqueous solution) was only able to solubilize about 33% of the initial amount of valrubicin (1mg) fed into the incubation mix. As reducing HSA has been shown to increase the affinity of HSA to lipophilic drugs such as paclitaxel (F. Chen et al., 2016; Wang, Huang, Zhao, Shao, & Cheng, 2013), the hypothesis was that partial reduction of HSA by breaking intramolecular disulfide bonds will result in an increase in valrubicin transportability and thus, an increase in valrubicin solubility in the aqueous environment. The rationale was that the additional free sulfhydryl groups of the reduced HSA (rHSA) will mediate the interaction between HSA molecules and provide opportunity for intermolecular interaction resulting in the self-assembly of HSA molecules. The self-assembly process will render accessible new hydrophobic sites for valrubicin binding (Fig. 9).

As previously mentioned, Cremophor EL is the current solvent for valrubicin. However, Cremophor EL is a toxic solvent that can exacerbate drug side effects upon systemic delivery. While testing additives to enhance valrubicin solubility in normal HSA, TPGS stood out as the only additive that could dissolve valrubicin as a single agent (Fig 10). In addition, TPGS has a

much wider application range compared to Cremophor EL in terms of administration routes. Whereas Cremophor EL is mostly used for intravenous and intravesical infusion, TPGS is used for oral, intraperitoneal, topical administration (Strickley, 2004). Moreover, during the several *in vivo* studies investigating TPGS-based drug formulation administered intravenously, there have been very few reports of off-target effects resulting from TPGS alone.

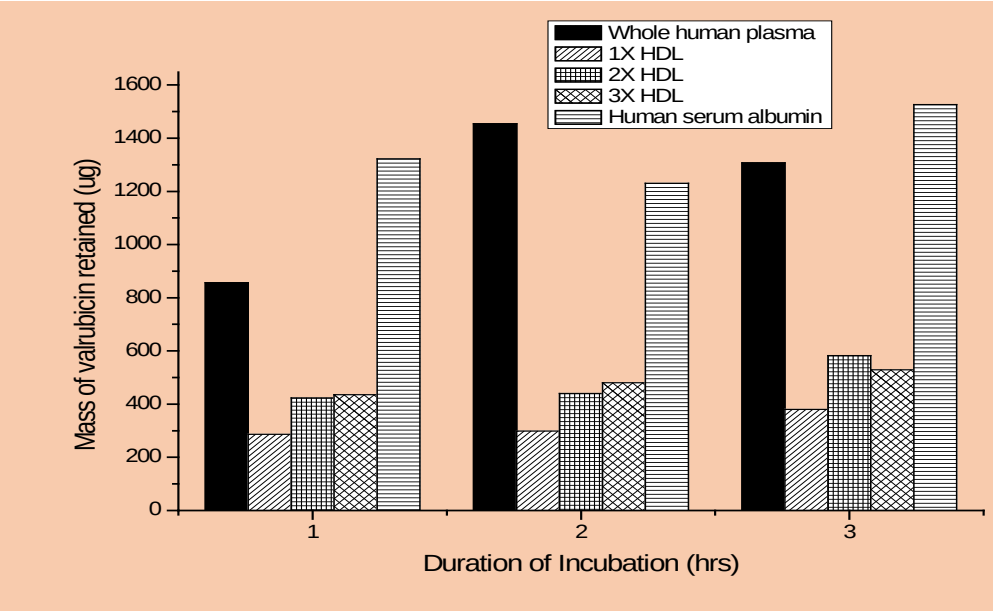

Figure 8: Time Course Study of Association of Valrubicin with Isolated Plasma Components and Whole Human Plasma. For this preliminary study with a feeding amount 5 mg (5000 μg) valrubicin in each of the plasma components, the highest valrubicin retention (about 30 %) after centrifugation was seen with whole human plasma and albumin for each additional hour of incubation.

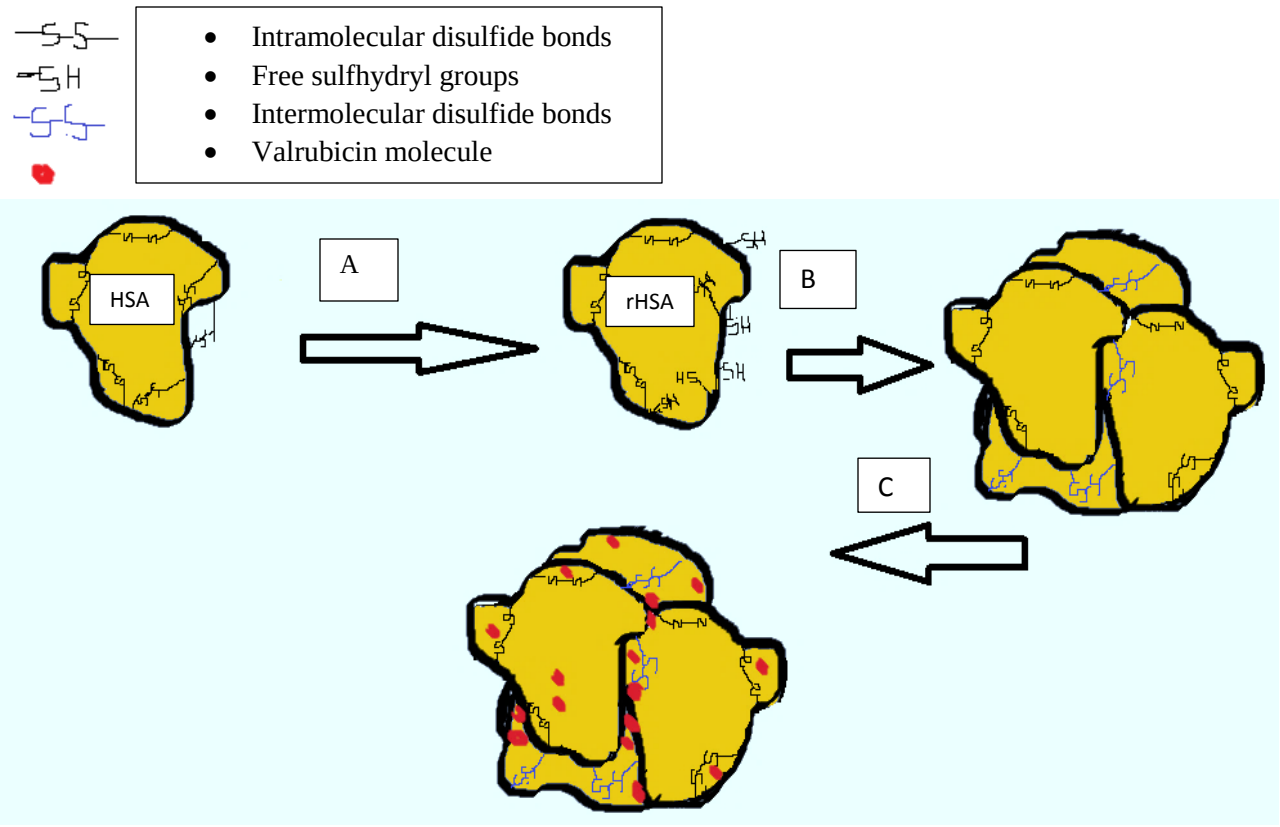

Figure 9: Schematic Representation of Preparation of Reduced HA using DTT. A) Partial reduction of disulfide bonds in HSA using dithiothreitol (DTT). B) Formation of intermolecular disulfide bonds that results in self-assembly of HSA molecules. C) Valrubicin molecules binding in the hydrophobic sites in the self-assembled HSA molecules.

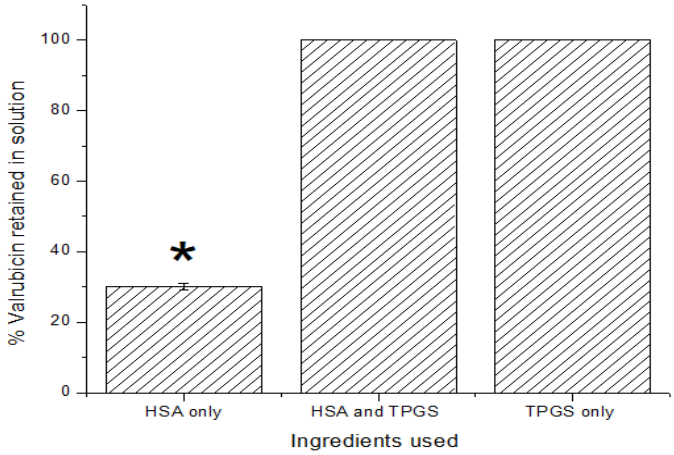

***Figure 7**: Effect of Using TPGS as An Additive to HSA on Valrubicin Solubility*

Specific Aim I: Preparation and Characterization of a Suspension of Valrubicin in Reduced Human Serum Albumin

This first project aimed to assess the feasibility of increasing the solubility of the hydrophobic anticancer drug valrubicin using human serum albumin (HSA) via a prior partial reduction of HSA. For this study, the rationale was that the broken disulfide bonds in reduced HSA will result in an altered configuration of HSA and thus may promote intermolecular interaction of HSA molecules. In the process of self-assembly, more hydrophobic binding sites on HSA could be accessible for valrubicin, and this was anticipated to produce an increase in valrubicin transportability.

Specific Aim II: Preparation and Characterization of Valrubicin-Loaded TPGS Micelles

The goal of this second project was to characterize the interaction of TPGS (D-alpha-tocopherol polyethylene glycol 1000 succinate) with valrubicin. Given that TPGS is a well-known solubilizer used in a wide array of drug delivery systems, especially for poorly water-soluble drugs via micelle formation, TPGS micelles could be potential carriers for valrubicin in an aqueous environment.

Overall Significance

Anthracyclines such as doxorubicin are potent anticancer drugs, and because they are relatively water- soluble and can be administered intravenously, their application in clinical practice extends to a several solid tumors and hematologic cancers. However, cardiotoxicity remains a major concern as doxorubicin (and other anthracycline to a lesser extent) can cause acute and delayed onset of cardiovascular damage, especially for in childhood cancer survivors. As a semi-synthetic derivative of doxorubicin, valrubicin has been shown to be much more effective and less toxic than its parent compound doxorubicin during pre-clinical studies.

However, the current formulation of valrubicin is restricted to the treatment of CIS-BCG bladder cancer and may only administered through intra-vesical instillation mainly due to the lipophilicity of the drug and the toxicity of the solvent (cremophor EL). A valrubicin formulation using biocompatible excipients such as HSA or TPGS could increase the solubility of valrubicin in an aqueous environment and extend its administration to alternative routes including systemic delivery. Valrubicin could then be used for other types of cancer in addition to CIS-BCG bladder cancer, and thus may offer a safer therapeutic alternative for anthracycline-based cancer chemotherapy.

CHAPTER II

MATERIALS AND METHODS

Time Course Study of Valrubicin Retention in Isolated Plasma Components

First, high density lipoproteins (HDL) were isolated from pooled human plasma by potassium bromide density gradient ultracentrifugation using a Beckman LE-80K ultracentrifuge and a Beckman SW40 Ti rotor, (22 hours, 256136.1g or 38,000 rpm). The HDL isolated after centrifugation was termed 1X HDL (1.7 mg/mL total protein concentration and 52 mg/dL total cholesterol content), and the 1X HDL was concentrated to 2X and 3XHDL sing polyethylene glycol. Protein content and cholesterol content were monitored using respectively a bicinchoninic acid (BCA) assay (Pierce) and a T-cholesterol E assay (Wako Diagnostics, Wako life Sciences). Fatty acid free, Globulin free HSA powder (Sigma Aldrich) was used to prepare a 45 mg/mL solution in distilled water.

All samples were kept at 4^{o}C until used. A concentration solution of valrubicin (50 mg/mL) in dimethyl sulfoxide (DMSO) was added to 1 mL of each plasma components to achieve a feeding concentration of 5000 μg/mL. Then, the samples were incubated at room temperature (RT) for a cumulative time of 3 hours. After incubation, the samples were centrifuged (3,000 rpm, 3 min) to remove unbound valrubicin. Absorbance at 490 nm taken on the supernatant using a spectrophotometer and fitted to a standard curve to determine the valrubicin retained in solution.

Preparation of an HSA-Valrubicin Suspension using TPGS as an Additive

Since TPGS is a known solubilizer, trial with an arbitrary amount of TPGS was undertaken to investigate its effect on the HSA-valrubicin suspension. To a fresh solution of 45 mg/mL HSA (Sigma Aldrich, fatty acid free, globulin-free), 1 mg of valrubicin was added (from a concentrated stock in DMSO). The mixture was stirred for 10 mins at RT after which 5 mg of TPGS (from a concentrated stock in distilled water) was added to the suspension for a final volume of 1 mL. The whole mixture was incubated at RT for 1 hour under constant stirring. As a control, an HSA-valrubicin suspension was prepared as described above with no addition of TPGS. For the TPGS-valrubicin sample, 1 mg of valrubicin (from a concentrated stock in DMSO) was added to fresh solution of 5mg/mL TPGS for a total volume of 1mL. The mixture was stirred at RT for 1 hour. After incubation, the three samples were centrifuged (3,000 rpm, 3min, VWR Galaxy 16) to remove unbound valrubicin. Absorbance at 490 nm was used to determine the amount of valrubicin retained in solution.

Specific Aim I: Preparation and Characterization of a Suspension of Valrubicin in Reduced Human Serum Albumin

Although the preliminary studies were performed with 45 mg/ml HSA to match the average HSA concentration in the blood, it is important to determine an optimal HSA concentration for these preparations described below. Since the preparations were expected to lead to the formation of nanoparticles, particle diameter size, polydispersity index, zeta potential, drug entrapment efficiency, *in vitro* release profile are parameters that will be assessed. These characterizations are essential since they relate to the suitability of nanoformulations for biomedical applications.

Determination of Optimal HSA Concentration for Valrubicin

Seven concentrations of HSA in distilled water were prepared (0, 5, 10, 20, 50, 75, 100 mg/mL). Then, a concentrated stock of valrubicin in DMSO (100mg/mL) was added to 1mL of each HSA solution to achieve an initial concentration of 0.5 mg/mL. After 2 hours of incubation at RT with constant stirring, the mixtures were centrifuged at 3,000 rpm for 3 mins, absorbance at 490 nm was taken on the supernatant using a spectrophotometer (Biotek, Cytation 3) to determine valrubicin retention in each solution.

Validation of HSA Reduction

Reduction of HSA was achieved using dithiothreitol (DTT). Briefly, a fresh solution of 100 mM DTT was prepared and added accordingly to 20 mg/mL HSA in a buffer solution (100 mM Tris base, 5mM ethylenediaminetetraacetic acid (EDTA), pH 8.4) to achieve final concentrations of 0, 0.5, 1, 2.0, 3.5, 5 and 7.5 mM DTT. These concentrations were chosen to maintain rHSA in solution. A high concentration of DTT could completely reduce the HSA which would assume a linear form of HSA with free sulfhydryl exposed. These linearized protein molecules would tangle and form protein fibrils that will precipitate out of the solution, creating a gel-like matrix.

The mixture was stirred at 37^{o}C for 1 hour. A desalting column (Sephadex PD10) with 5mM EDTA (pH 7) as an elution buffer -to maintain the stability of free sulfhydryl groups)- was used to separate the protein content of each mixture from excess DTT. Then, a BCA reagent kit (Thermo Scientific Pierce) and a 5,5-dithio-bis-(2-nitrobenzoic acid) (DTNB, Sigma Aldrich) assay were respectively used as per manufacturer recommendations to determine the protein and free sulfhydryl content of each elution fraction. Excess DTT elution was also determined using the DNTB assay since DTT has two sulfhydryl groups in its structure. The reduction percent was calculated using the theoretical total free sulfhydryl group (obtained by multiplying the moles of

free sulfhydryl groups in unreduced HSA by 35) as 100% reduction. Additionally, the tryptophan emission spectra of the reduced and normal HSA were acquired from Cary Eclipse spectrofluorometer (Varian Inc., Australia, excitation wavelength 295 nm, emission wavelength range 300-500 nm) for comparison.

Preparation of rHSA-Valrubicin Suspensions

The rHSA-valrubicin suspensions were prepared by a simple method of dissolution. Briefly, a fresh solution of DTT was added to 20 mg/mL HSA in a buffer solution (100 mM Tris base, 5mM ethylenediaminetetraacetic acid (EDTA), pH 8.4) to achieve final concentrations of 0, 0.5, 1, 2.0, 3.5, 5 and 7.5 mM DTT. Each mixture was stirred at 37^{o}C for 1 hour. A limitation of this preparation is the high fold dilution of using a desalting column to remove excess DTT. Hence, the final HSA collected as a fraction may be too diluted to retain valrubicin in solution. Thus, instead of using a desalting column, dialysis is an alternate option that works as well. After incubation, the mixture was dialyzed against deionized water (Spectrum Labs, 6000-8000 kDa molecular weight cut-off) for 24 hours at 4^{o}C. A 100 mg/mL stock of valrubicin in DMSO was added to the reduced HSA, and again, the mixture was incubated with stirring at RT for 2 hours. Unbound valrubicin was removed after centrifugation at 3,000 rpm for 3 min. Absorbance at 490 nm was taken on the supernatant using a spectrophotometer (Biotek, Cytation 3) to determine valrubicin retention in each suspension.

Determination of Valrubicin Entrapment and Loading efficiency

The drug entrapment efficiency (DEE) was calculated using this formula below:

DEE= {Amount of valrubicin retained after centrifugation} x 100/ {Feeding amount of valrubicin}

The feeding amount of valrubicin as previously mentioned is 0.5 mg for 1 mL of mixture. The drug loading efficiency (DLE) was calculated using this formula below:

DLE= {Loaded drug mass}x 100/ {Total mass of components of the formulation}

Particle Diameter Size, Polydispersity and Zeta Potential Measurement

Dynamic light scattering (DLS) which measures changes in the intensity of light scattered by particles as a function of time was used to access particle diameter size of the rHSA-valrubicin suspension with 3.5 mM DTT. DLS was also used to measure the polydispersity index (PDI) which is a measure of homogeneity and size distribution the preparation. Briefly, 100 µL of the rHSA-valrubicin suspension was diluted 1500 µL with deionized water in a cuvette which was placed in a Beckman Coulter Delsa Nano particle analyzer for measurement The zeta potential is the effective surface charge of the particles in solution, and is used often to indicate stability levels of colloidal solution (Bhattacharjee, 2016). Malvern Instrument zetasizer was used to determine the zeta potential.

Transmission Electron Microscopy

In transmission electron microscopy (TEM), a beam of electrons is precipitated through a sample placed on a grid, and the interaction of the electrons with the grid and the sample forms the image of the sample. In this study, the dialyzed suspension of rHSA -valrubicin was diluted 20 times with double distilled water. Then, a drop of the sample was placed on a discharged Formvar carbon coated 200 copper mesh grid (Electron Microscope Sciences) and left to dry for 1 min. Then, the sample was negatively stained with a drop of 2% uranyl acetate for 1 min. The sample was visualized using FEI Tecnai G2 Spirit Biotwin transmission electron microscope.

In Vitro Release Studies

A dynamic dialysis technique was used to perform the *in vitro* release study assesses the integrity of the drug carrier. Briefly, 2mL of the rHSA-valrubicin suspension was pipetted in a dialysis bag (Spectrum Labs, 6-8 kDa molecular weight cut off), and placed in 50 mL of 1X phosphate-buffered saline enhanced with 5% tween 20 (pH 7.4). This setup was shaken (120 rpm) in a gyratory incubator shaker (INNOVA 4300, New Brunswick Scientific) at 37^{o}C for a cumulative time of 96 hours. At selected time intervals, the outside buffer was sampled, and the same volume of fresh buffer was added as a replacement. The same treatment was given to valrubicin dissolved in 90% cremophor/10% ethanol. Each sample of buffer taken was analyzed for traces of valrubicin using fluorescence intensity measurement (Biotek, Cytation 3).

In Vitro Cytotoxicity Studies

A malignant ovarian cancer cell line (HeyA8), a "normal" immortal ovarian epithelial cell line (HIO180) were selected due to the reported sensitivity of ovarian cancer cells to albumin-bound chemotherapy (J. Chen et al., 2012). Both cell lines were graciously provided by MD Anderson Cancer Institute and used in respectively passage 6 and 5. A cell counting kit (CCK-8, Dojindo) was used to investigate cell survival after treatment with the rHSA-valrubicin formulation. Briefly, the cells were cultured in RPMI 1640 medium (Gibco) supplemented with 10% fetal bovine serum (Hyclone) and 1% penicillin streptomycin (Gibco). At 90% confluence, the cells were trypsinized with 0.25% trypsin EDTA (Gibco)and counted using a Cellometer mini (Nexcelom). Five thousand cells were plated per well in a 96-well plate and incubated overnight. Next, the cells were treated with the DMSO, rHSA alone, rHSA-valrubicin and free valrubicin (valrubicin dissolved in DMSO) for 48 hours, Absorbance at 450 nm was measured after addition of 10 μL of CCK-8 reagent to each well and a 3- hour incubation at 37^{o}C. The IC_{50}

(concentration of formulation resulting in 50% of cell death) was determined from the survival curve generated.

Specific Aim II: Preparation and Characterization of Valrubicin-Loaded TPGS Micelles

Determination of The Critical Micelle Concentration

The critical micelle concentration (CMC) is the concentration of the surfactant in solution at which micelles start forming. Although the CMC of TPGS at 37 degrees in PBS has been reported in the literature to be 0.2 mg/mL (Guo et al., 2013), such a value is dependent upon the conditions of the experiments, temperature included. Thus, the CMC for the conditions of preparation of TPGS-valrubicin (RT) was determined. Briefly, the same amount of valrubicin (5 μg) was added to 1 mL of different concentrations of TPGS (from 0 to 5 mg/mL). Then, fluorescence spectrum emission of valrubicin (excitation wavelength 485 nm, emission wavelength range 500-620 nm) measurements were taken on each sample using Cary Eclipse spectrofluorometer (Varian Inc.).

As a direction -dependent property, anisotropy is inversely related to the rotational motion of particles. Since larger particle will rotate slower than a smaller one, anisotropy can be used as a tool to investigate the interaction of a fluorophore such as valrubicin with its immediate environment. In this study the anisotropy of each TPGS-valrubicin sample was assessed using a manual polarizer in the Cary Eclipse spectrofluorometer. The formula below was used to calculate the anisotropy:

$$r=(I_{VV} GI_{VH})/(I_{VV}+ 2GI_{VH})$$ (S. Shah et al., 2016)

Where r is the anisotropy, I is the fluorescence intensity taken in different planes, VV: vertical-vertical plane, VH: vertical-horizontal plane, and the G factor is the ratio of I_{HV} to I_{HH}.

Evaluation of Valrubicin Solubility in TPGS

At set amount of valrubicin (0.5 mg from a concentrated stock in DMSO) was added to 1mL increasing concentrations of TPGS. Each mixture was continuously stirred at RT for 1 hour after which each mixture was centrifuged at 10, 000 rpm for 10 min. Absorbance at 490 nm was taken on the supernatant to determine the percent valrubicin retention in solution.

Preparation of Valrubicin-Loaded TPGS micelles

A simple thin-film, solvent casting method was used for the preparation of valrubicin-loaded TPGS as described by Muthu et al. with some modifications. Briefly, 2.4 mg of TPGS wax and 0.5 mg valrubicin powder were dissolved in 200 μL chloroform. Then, the chloroform was evaporated under nitrogen in a rotatory motion. The sample was further placed in the water bath at 37^{o}C for 1 hour to ensure total removal by evaporation of the chloroform. Then, distilled water was used to reconstitute the thin film. The mixture was allowed to stir at RT for 1 hour. The mixture was then filtered through a syringe filter 0.22 μm cut off pore size to remove unbound valrubicin. Absorbance at 490 nm on the filtrate was used to check percent valrubicin retention in the solution.

Determination of Drug Entrapment Efficiency

The same formula previously described for the rHSA- valrubicin was applied to the TPGS-valrubicin after determination of the percent valrubicin retention.

Particle Diameter Size, Polydispersity Index, Zeta Potential Measurement and Transmission Electron Microscopy

These characterization procedures were performed as described for rHSA-valrubicin preparation with some modifications. Due to the anticipated small size of the TPGS micelles, the Malvern Instruments zetasizer- which can distinguish < 1000 Da molecules and < 1 nm particles-

was used for diameter size, PDI and zeta potential measurement on the TPGS-valrubicin sample which remained undiluted. For the TEM, the TPGS-valrubicin sample was diluted to half concentration with double distilled water and placed on a lacey Formvar carbon-coated 300 mesh copper grid (TED PELLA, Inc.).

In Vitro Release Studies and In vitro Cytotoxicity Studies

These studies were performed as previously described for the rHSA-valrubicin.

Statistical Analysis

At the exception of preliminary studies, each sample preparation and characterization were done at least three times in independent experiments and standard deviation (SD), or standard error of the mean (s.e.m.) was reported. One way-ANOVA with Tukey post- hoc test was used for comparison (Origin Labs software).

CHAPTER III

RESULTS

HSA Reduction Using DTT

The valrubicin retention in normal HSA solution was dependent upon HSA concentration until the concentration of 20 mg/mL HSA was reached. Hence, 20 mg/mL or to higher HSA concentration was able to retain 64.3 % of the initial 0.5 mg of valrubicin used in the incubation mix (Fig 11). Thus, 20 mg/mL rHSA concentration was used in the subsequent experiments.

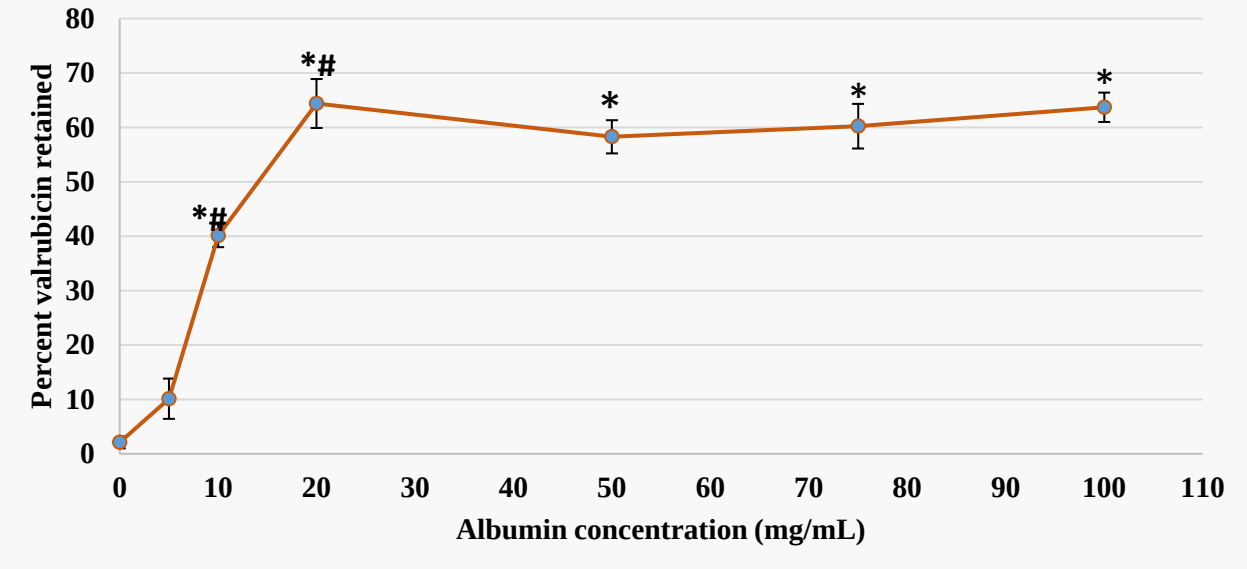

Figure 8: Optimal Concentration of HSA for Valrubicin Retention. Values ± SD. One-way ANOVA followed by *post hoc* Tukey's test (* P<0.01 when compared to 0 mg/ml albumin, # p< 0.01 when compared to the precedent albumin concentration).

A desalting column was effective in separating the DTT from HSA (Fig 12-16). Under the stated conditions, the highest reduction efficiency (57.3%) was achieved upon treatment of 20 mg/mL with 5mM DTT (Fig. 17). Interestingly, the fluorescence emission spectrum of rHSA compared to normal HSA showed a blue shift of 7 nm (340nm shifted to 333 nm) and a lower fluorescence intensity (Fig. 18) when usually, reduced HSA shows a red shift (Young Lee & Hirose, 1992).

Effect of HSA Reduction on Valrubicin Solubility

Of all rHSA-valrubicin suspensions, only the rHSA-valrubicin made with 3.5 mM DTT showed a significant increase in valrubicin solubility: 85.4 % valrubicin retention compared to the 51% valrubicin retention of normal HSA (Fig 19).

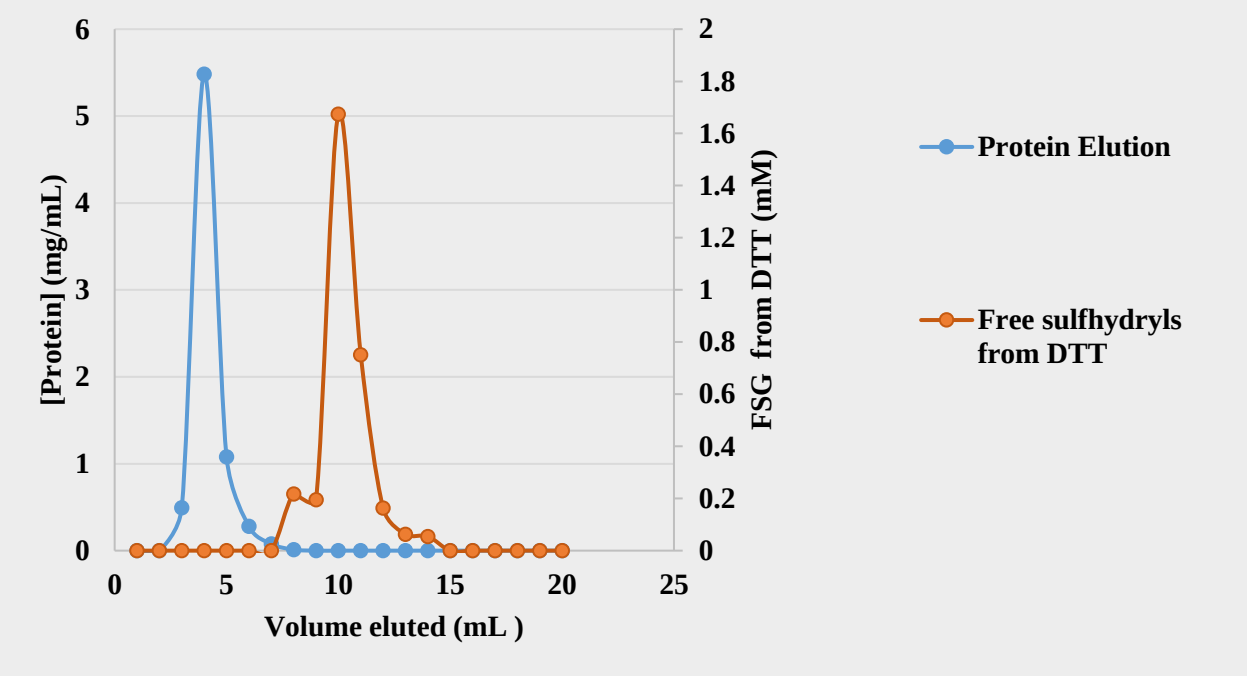

Figure 9: Independent Elution Pattern of HSA and DTT on Sephadex PD 10. Here, HSA and DTT were run on the column in two separate runs, and their elution patterns were merged to show elution separation. FSG = free sulfhydryl groups.

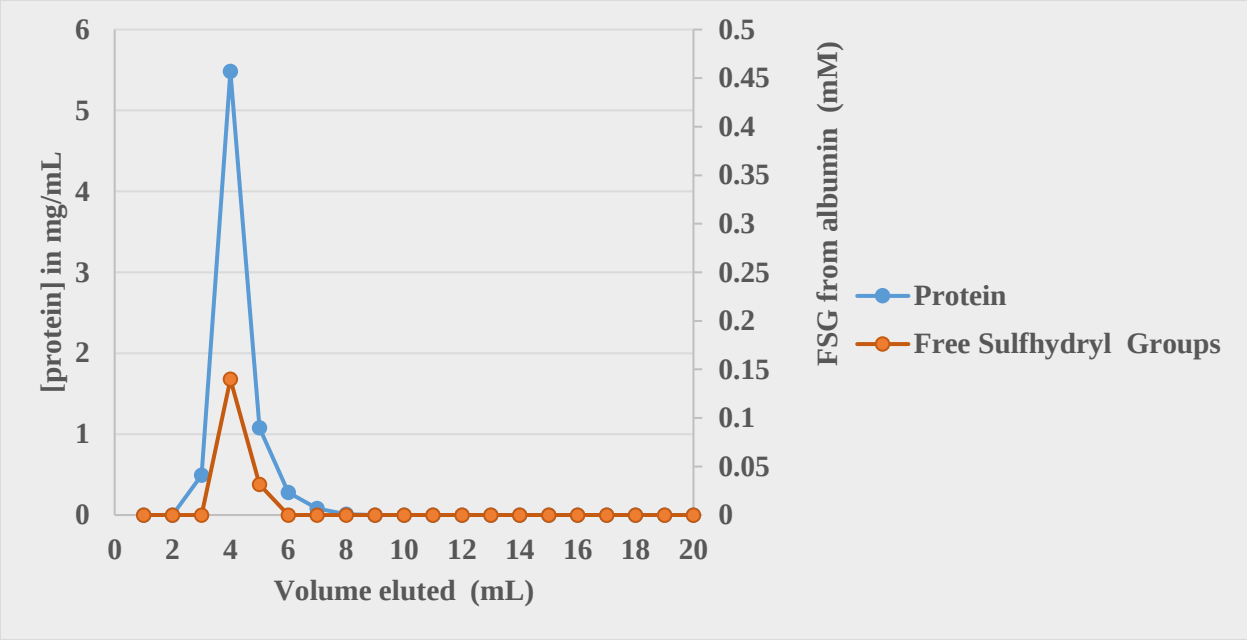

Figure 10: Free Sulfhydryl Groups Present in Normal HSA Eluted. Here, a DTNB assay followed the protein quantification BCA assay to determine baseline FSG content in normal HSA eluted.

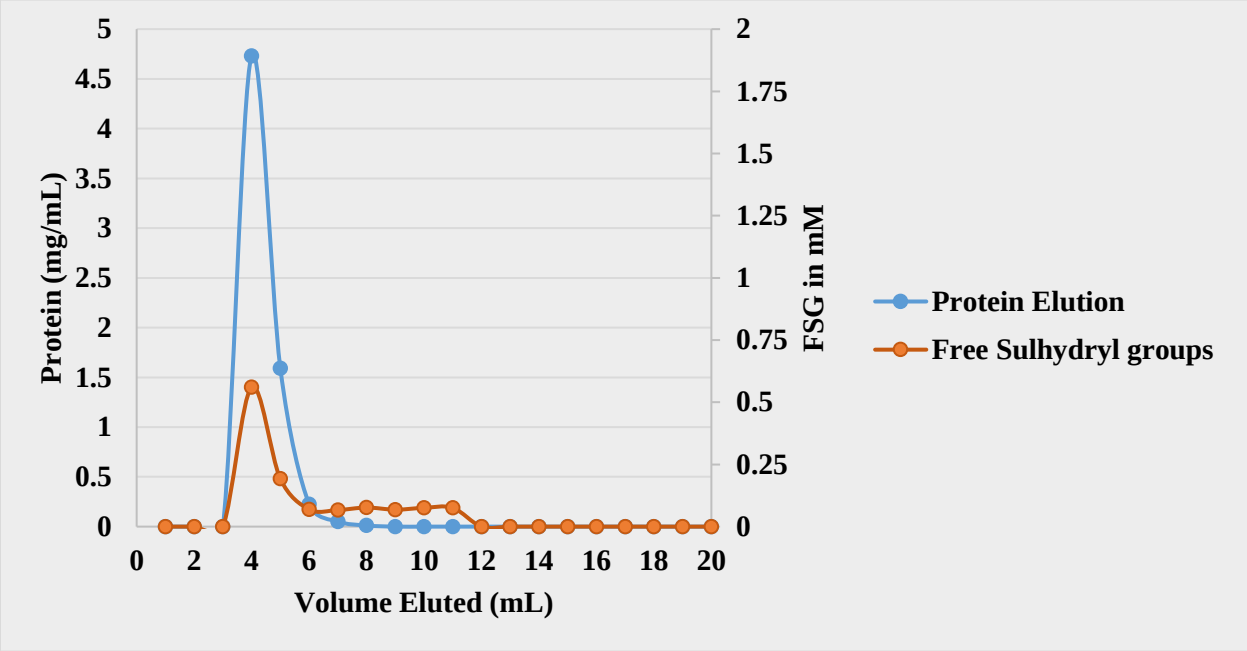

Figure 11: Elution Pattern of rHSA using 1mM DTT.

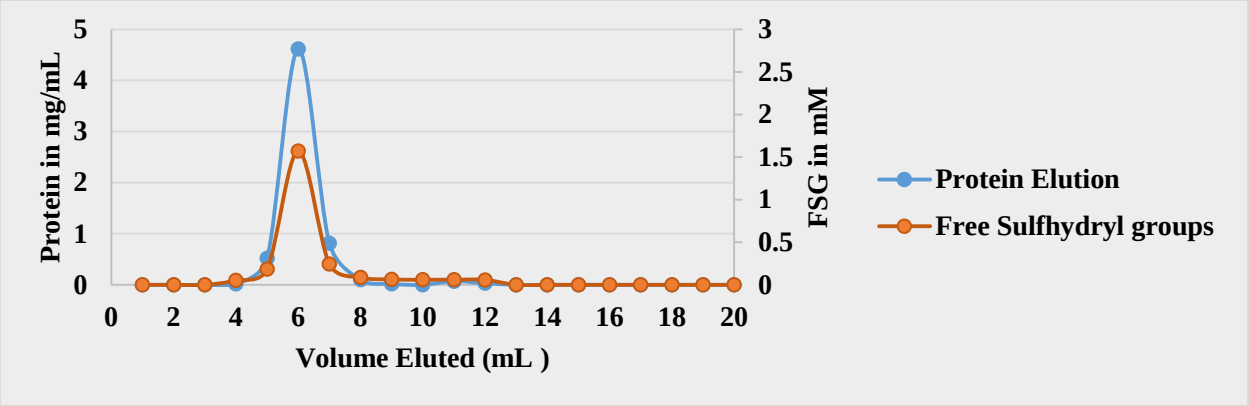

Figure 12: Elution Pattern of rHSA using 3.5 mM DTT.

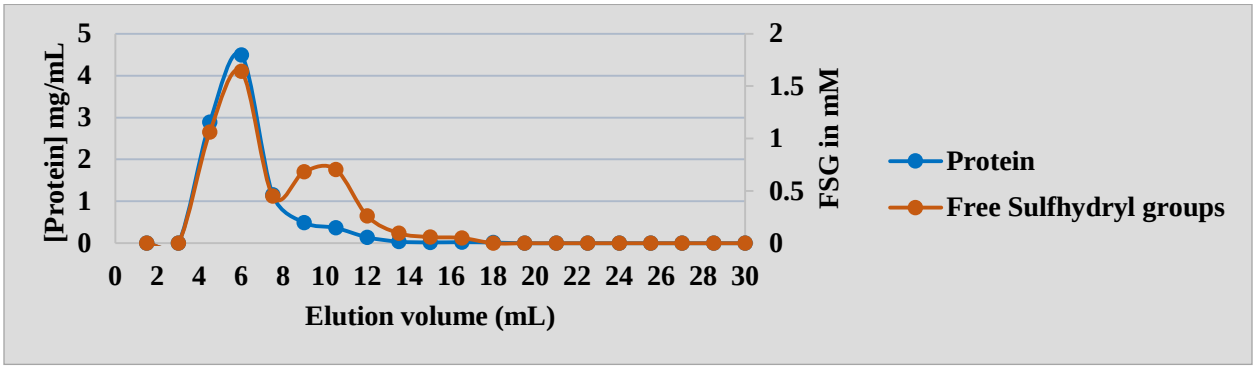

Figure 13: Elution Pattern of rHSA using 5.0 mM DTT. Excess unreacted DTT started eluting at fraction 9.

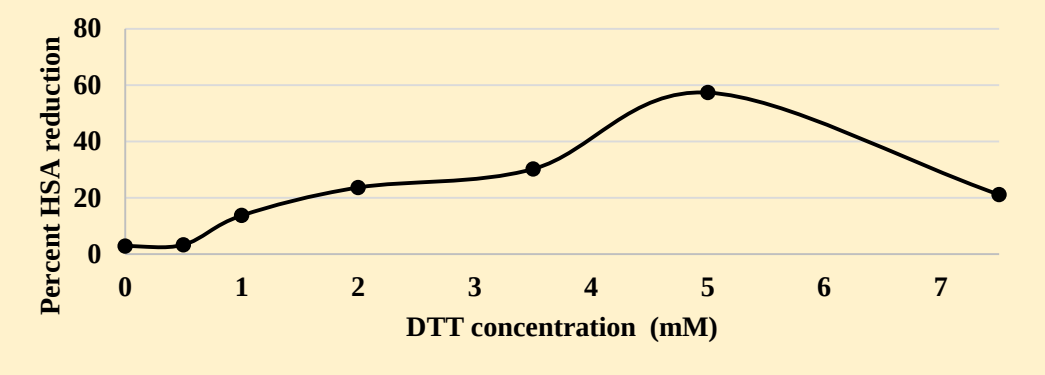

Figure 14: HSA Reduction Efficiency upon DTT Treatment.

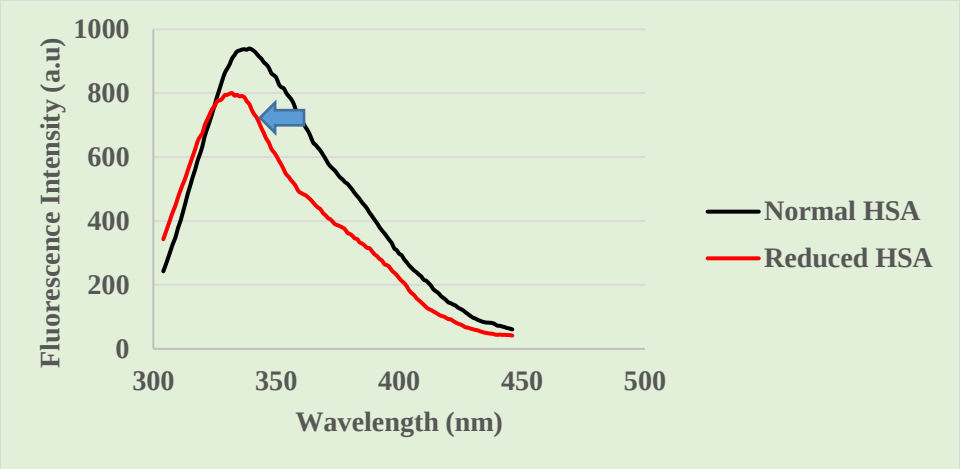

Figure 15: Fluorescence Emission Spectra of Normal HSA and rHSA. The arrow shows the shift to the left (also termed as blue shift) in the albumin emission spectra upon partial reduction.

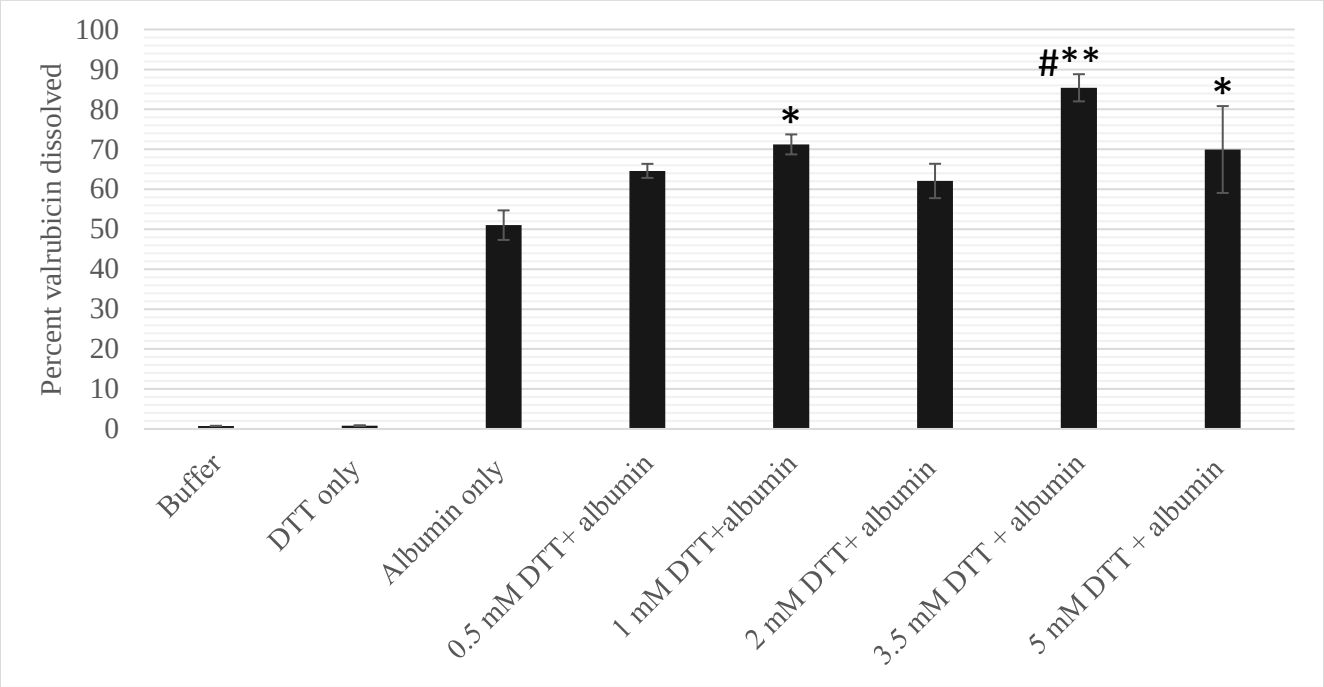

Figure 16: Effect of Reducing HSA on Valrubicin Solubility: Values± SD. *p<0.05, ** p< 0.01 (One -way ANOVA followed by Tukey's test) statistically greater than Albumin only group. # p <0.01 (ANOVA followed by *post hoc* Tukey's test) statistically greater than all other previous groups.

Characterization of rHSA-Valrubicin

As previously mentioned, the DEE of rHSA-Val was 85.4% when 0.5 mg initial valrubicin was used in the incubation mix. The DLE was determined to be 2.1% while the major component of the rHSA-valrubicin was protein (Fig 20) The rHSA alone preparation presents as a translucent suspension similar to the rHSA-valrubicin suspension (Fig 21) As shown in Table 5, the average particle diameter size of rHSA-valrubicin was higher compared to a suspension on normal HSA and valrubicin as determined by DLS method (respectively 124.7± 37.9 nm and 67.83±10.8 nm). The PDI (a measure preparation homogeneity) also displayed as similar pattern: 0.332± 0.14 for rHSA-valrubicin and 0.290±0.03 for HSA-valrubicin. The TEM images showed a polydisperse particle population with diameter size ranging from 18 nm to 370 nm (measured from 5 different fields randomly selected). Surrounded by a corona, all particles looked fairly spherical (Fig. 22).

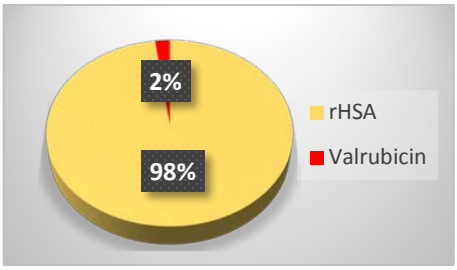

Figure 17: Chemical Composition of rHSA-Valrubicin.

In Vitro Release Studies and Cytotoxicity Studies on rHSA-Valrubicin

Compared to free valrubicin, rHSA-valrubicin shows as slower release profile. After 96 hours of incubation, only 5.15% of the entrapped valrubicin in rHSA-valrubicin were released from the dialysis bag whereas 85.6% of the free valrubicin formulation were released during the same time interval (Fig. 23). In cytotoxicity studies, the rHSA only treatment resulted in an increase in cell proliferation both for the malignant (ovarian carcinoma) HeyA8 cells and normal cells

(ovarian epithelial) HIO180 cells (Fig.24 and 25). However, HeyA8 cells were more sensitive (IC_{50} 6.9 ± 1.9 μM) than normal HIO180 cells (> 30μM) to rHSA- valrubicin while both cell lines were similarly affected by the free valrubicin (Table 6).

Table 5: Physicochemical Characterization of rHSA-Valrubicin. Values are means ± SD.

Samples	Size (nm)	PDI	Zeta Potential (mV)
HSA only	10.15± 1.04	0.192 ± 0.04	N/A
rHSA only	130.6± 1.87	0.424± 0.07	N/A
HSA-Valrubicin	67.83± 10.8	0.290± 0.03	-10.93± 0.5
rHSA-Valrubicin	124.7±37.9	0.332± 0.14	-19.03± 3.3

A **B** **C**

Figure 18: Pictures of rHSA alone and rHSA-Valrubicin. A) Normal HSA B) rHSA alone (using 3.5 mM DTT) C) rHSA-Valrubicin (using 3.5 mM DTT).

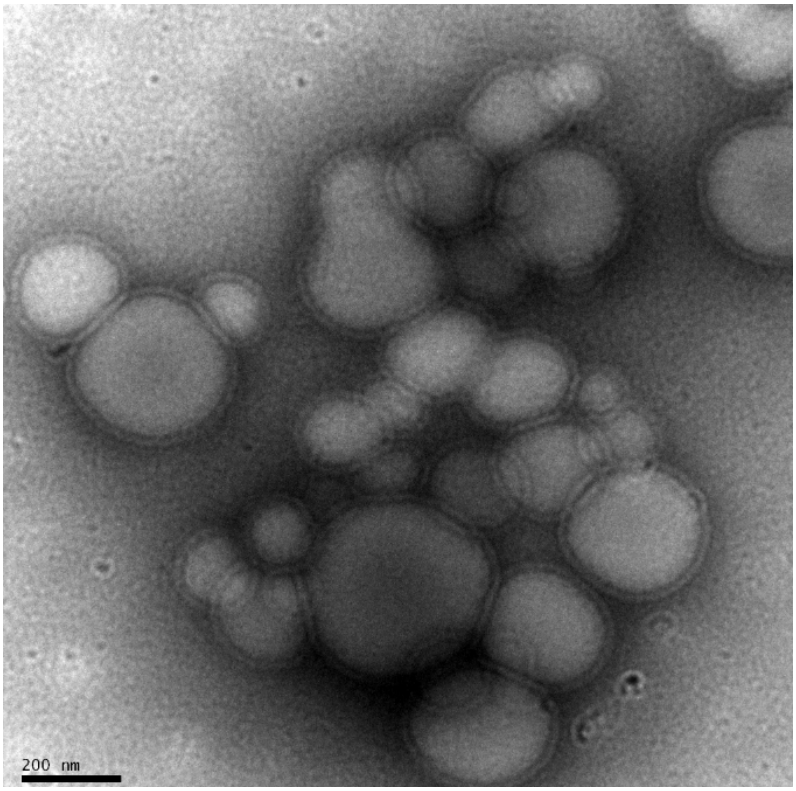

Figure 19: TEM Image of rHSA-Valrubicin Sample.

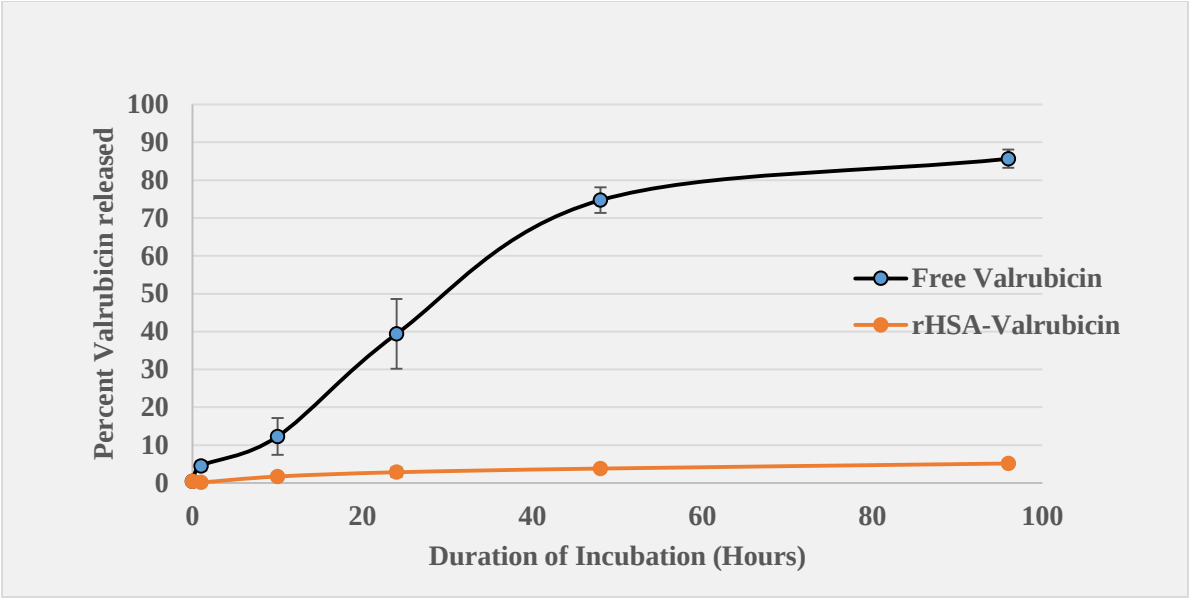

Figure 20: *In Vitro* release Profile of rHSA-Valrubicin.

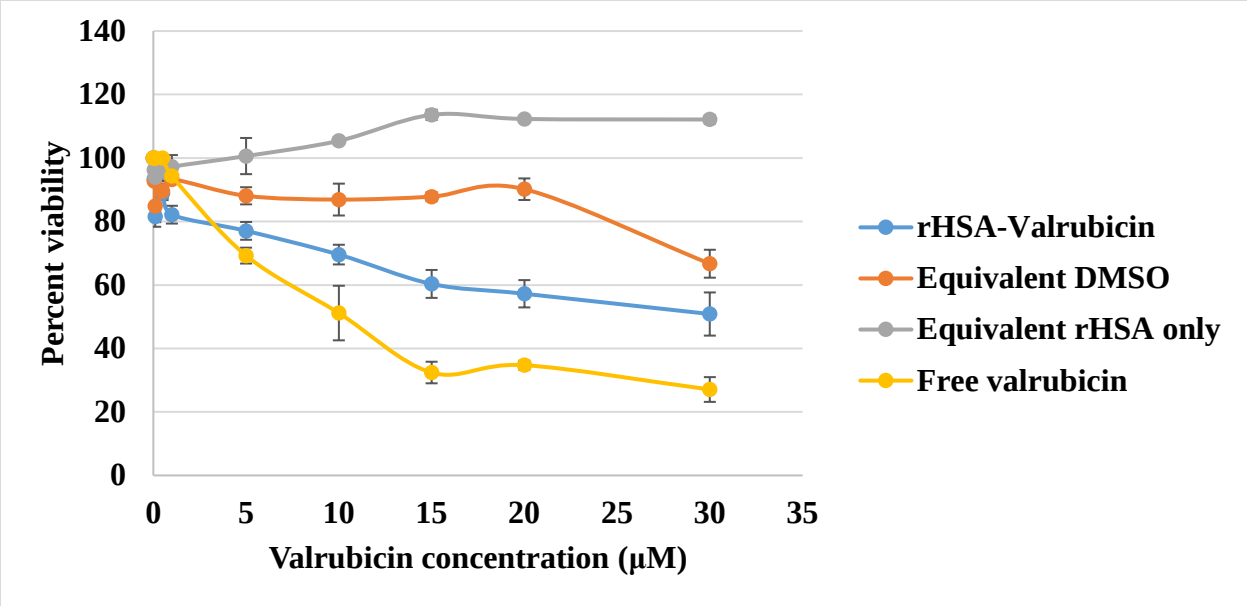

Figure 21: Effect on rHSA-Valrubicin Treatment on Percent Survival of HIO180 Ovarian Epithelial Cells. Bars represent standard error of the mean.

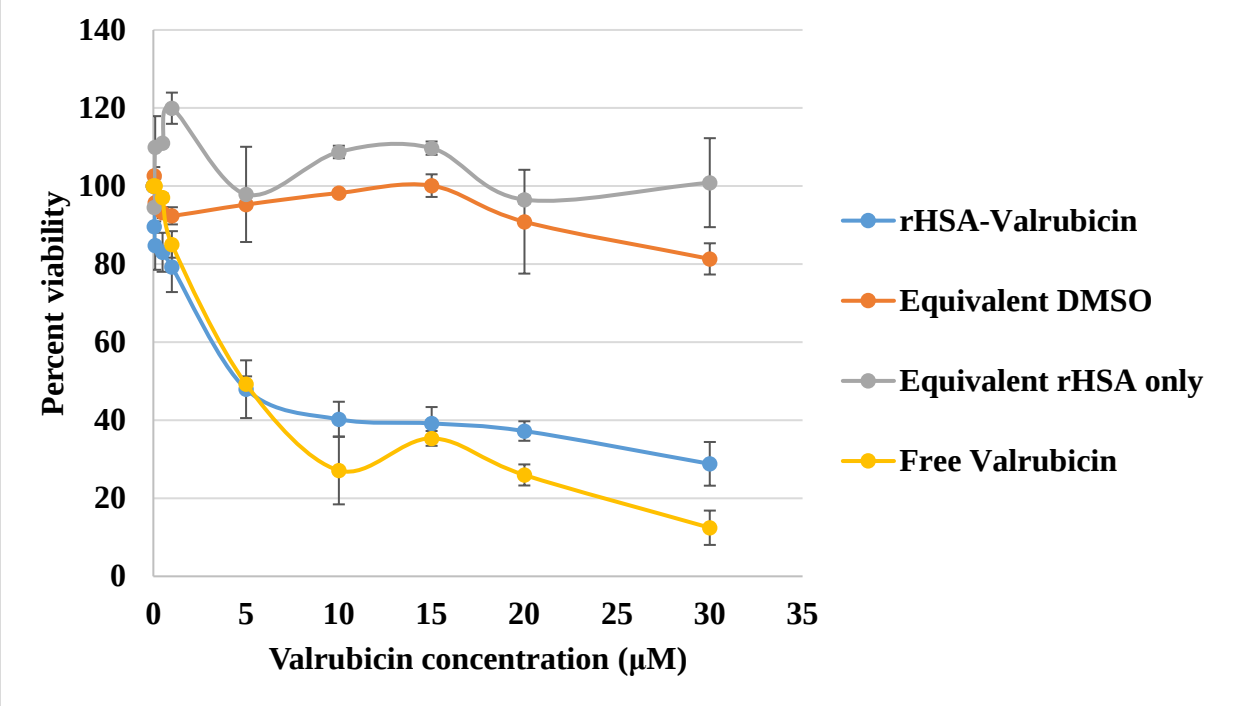

Figure 22: Effect on rHSA-Valrubicin Treatment on Percent Survival of HeyA8 Ovarian Malignant Cells. Bar represent standard error of the mean.

Table 6: IC_{50} Values from rHSA-Valrubicin Treatment. Values (μM) are ± SD.

Treatments	HIO180 (μM)	Hey A8(μM)
rHSA-Valrubicin	>30	6.9±1.9
Free Valrubicin	10.3± 1.4	9.13±0.14

Determination of Critical Micelle Concentration of TPGS and Valrubicin Solubility in TPGS

The CMC obtained from fluorometric anisotropy measurements was calculated to be 23 μM TPGS (Fig. 26). Intriguingly, the fluorescence from valrubicin molecules is quenched just before the CMC is reached and rises back up once the CMC is exceeded (Fig 27). A concentration of 2.4 mg/mL TPGS or higher was able to solubilize 0.5 mg valrubicin, and overall, the amount of valrubicin dissolved was strongly dependent upon TPGS concentration as 2.4 mg/mL TPGS was unable to dissolve 0.75 mg valrubicin (Fig 28).

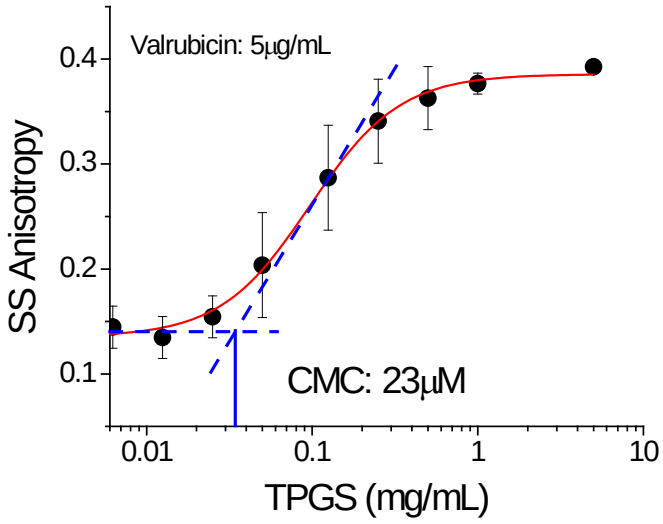

Figure 23: Anisotropy Measurements of TPGS-Valrubicin.

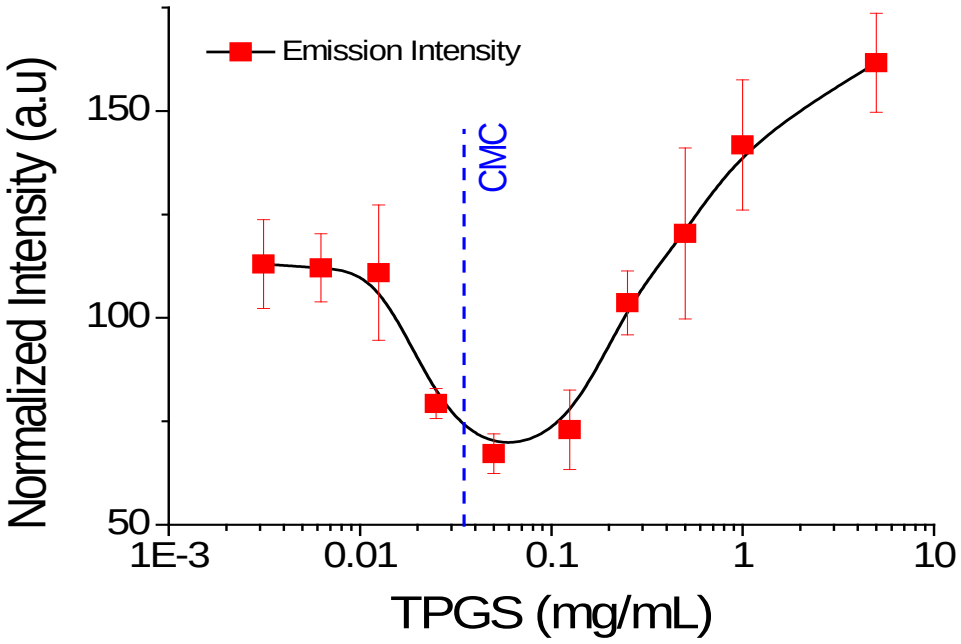

Figure 24: Change in Valrubicin Fluorescence Intensity with Increasing TPGS Concentration.

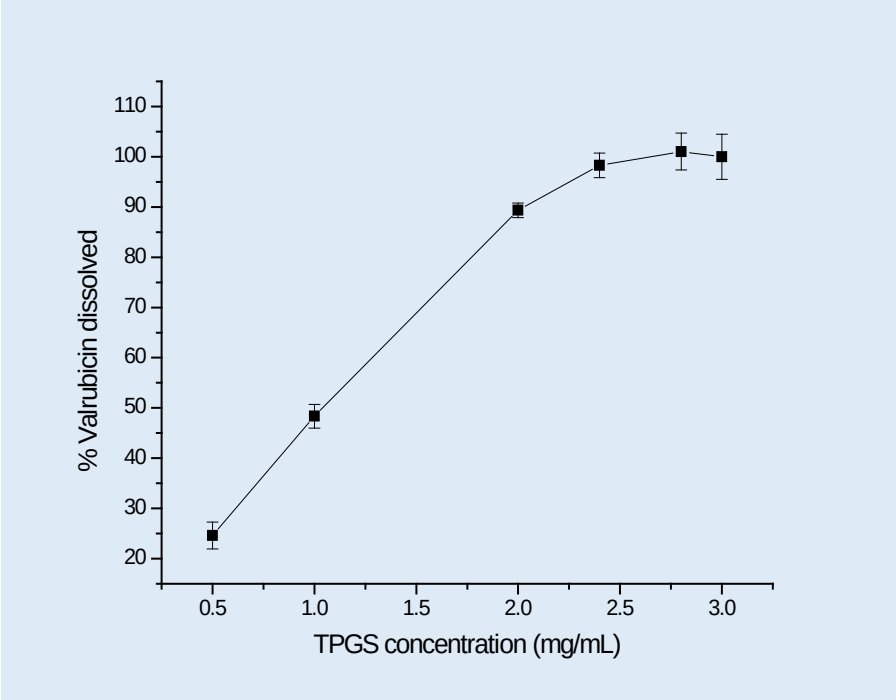

Figure 25: Effect of TPGS Concentration in Valrubicin Solubility.

Physicochemical Characterization of TPGS-Valrubicin Micelles

The TPGS-valrubicin preparation presents as a clear solution (Fig. 29). While the DEE for using 0.5 mg initial valrubicin amount for 2.4 mg TPGS in a total of 1 mL solution was about 100%, the DLE is about 17.3% valrubicin and 82.7% TPGS of the mixture is TPGS (Fig. 30). While the TEM image showed particles with diameter size ranging from 9 nm to 15 nm (Fig. 31), the DLS measurements revealed particle size of 13.2± 1.3 nm with a PDI of 0.188 ±0.001. The zeta potential was -1.94±0.72 mV (Table 7).

Figure 26: TPGS-Valrubicin Solution.

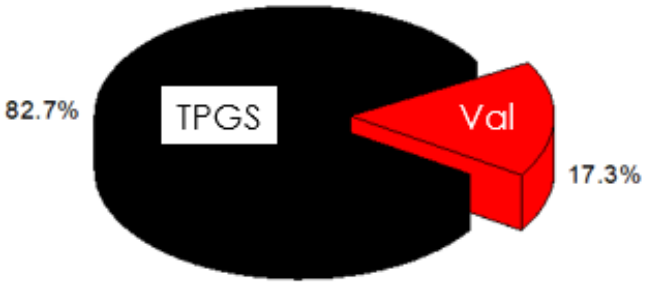

Figure 27: Chemical Composition of Valrubicin -Loaded TPGS Micelles.

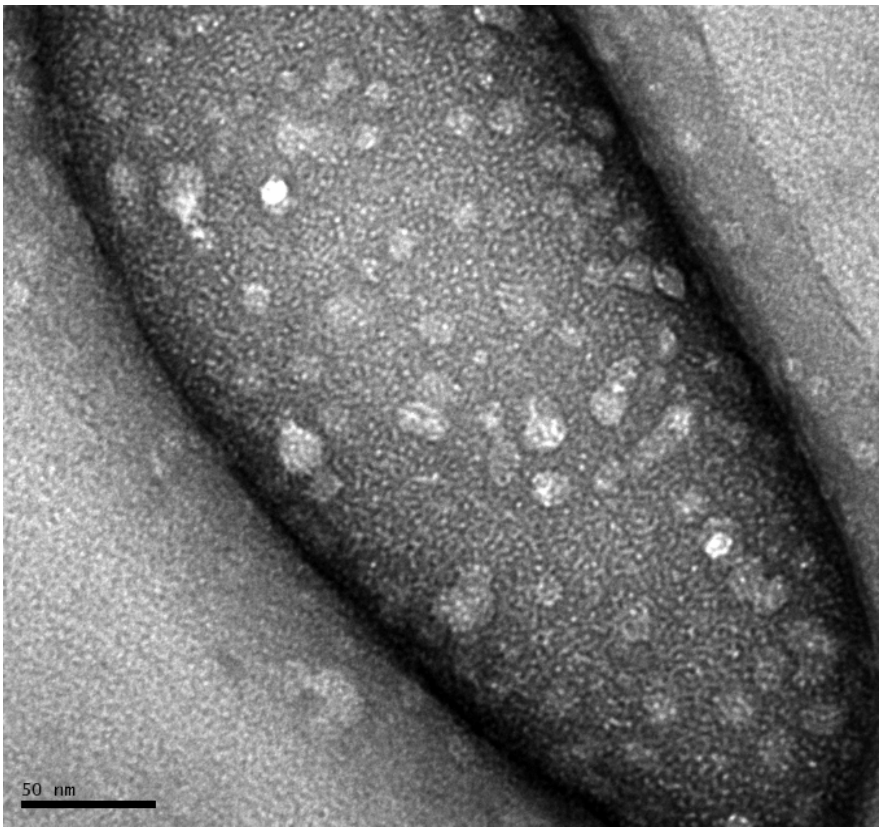

Figure 31: TEM Image of TPGS-Valrubicin Sample.

Table 7: Estimation of Diameter Size, PDI and Zeta Potential of TPGS-Valrubicin by DLS.

Samples	Diameter Size (nm)	PDI	Zeta Potential (mV)
TPGS only	11.61 ±0.9	0.028 ± 0.02	-0.284 ± 0.1
TPGS-Valrubicin	13.2 ± 1.3	0.188 ±0.001	-1.94 ± 0.72

In Vitro Release Studies and Cytotoxicity Studies on TPGS-Valrubicin

The TPGS-Valrubicin sample showed a slower release profile than the free valrubicin. Nearly 88.1% of the valrubicin was preserved in the TPGS micelles (inside the dialysis bag) during the 96 hours incubation time (Fig.32). In cytotoxicity studies, the TPGS-valrubicin did not exert a

protective effect on the HIO180 cells as the IC_{50} values are quite close to that of the free valrubicin. However, it was nearly three time as effective in killing the malignant HeyA8 cells compared to the free drug (Table 8).

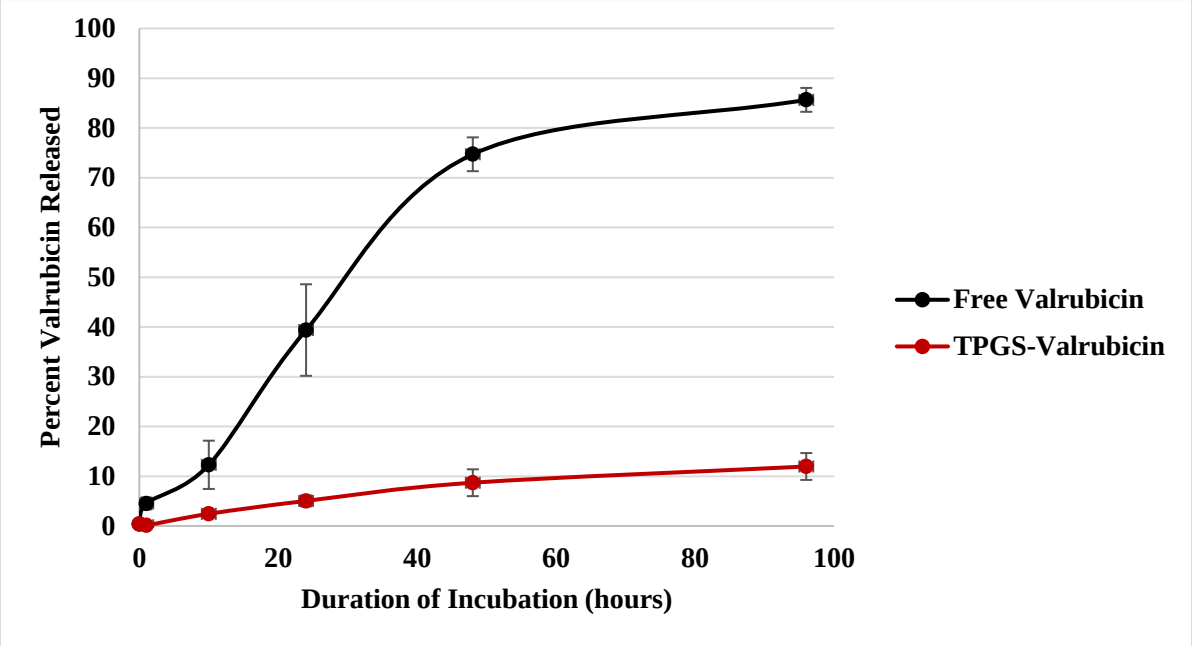

Figure 32: *In Vitro* Release Profile of TPGS-Valrubicin. Bars represent means ±SD.

Table 8: IC50 Values from TPGS-Valrubicin Treatment. Values (µM) are means ± SD.

Treatments	HIO180 (µM)	Hey A8 (µM)
TPGS-valrubicin	7.3±1.0	3.7± 1.1
Free valrubicin	10.3± 1.4	9.13± 0.14
TPGS only	47.5± 0.3	33.1± 2.2

CHAPTER IV

DISCUSSION

Aside from a cream-based formulation of valrubicin for psoriasis treatment in clinical trial (Hauge et al., 2012), there has been very few attempts to find an appropriate carrier for valrubicin for systemic delivery in cancer therapy. In this study, HSA and TPGS were separately assessed as valrubicin excipients that could potentially replace the current organic solvent of valrubicin: Cremophor EL. Owing to the already established desirable safety profile of valrubicin, a more biocompatible vehicle such as HSA or TPGS could extend valrubicin administration from intravesical to additional routes. Subsequently, valrubicin can serve as a safer option in anthracycline -based therapy which is still heavily used in different types of cancer, especially childhood blood cancers (*American Cancer Society*, 2016). For a poorly water-soluble drug like valrubicin, nanoparticles can offer a gateway into its broader use because nanoparticles made with biomaterials components could improve valrubicin's aqueous solubility with the potential added benefit of enhancing its bioavailability, of increasing its tumor accumulation and of further reducing off-target effects (Narvekar, Xue, Eoh, & Wong, 2014).

Diverse materials can be used as ingredients for nanoparticle assembly, however, biomacromolecules such as HSA offer the most advantages in a clinical setting. They are biocompatible, biodegradable, and they have inherent biochemical and structural properties that facilitate a longer circulatory life and targeting approaches (Y. Zhang et al., 2018). Several

animal studies have shown how different types nanoparticles, loaded with anticancer drugs, experience an enhanced permeation retention effect due to their small size, the leaky vasculature and low lymphatic drainage at the tumor site (Merlot et al., 2014). However, being an extravascular protein, HSA is uniquely suited as a vehicle for drugs targeting solid tumors as beside moving through fenestrations in between vascular endothelial cells, HSA uses receptor mediated mechanisms to move through these endothelial cells as well. These reasons contributed improving the efficiency of paclitaxel by 33% in the HSA-bound paclitaxel formulation marketed as Abraxane. Although they can produce adverse effects, surfactants easily promote solubility for hydrophobic drugs by forming micelles. In contrast, TPGS, a well-studied micelle-forming surfactant, is recognized as a safe nutritional supplement, especially as TPGS is derived from the naturally occurring vitamin E. These above-mentioned properties make TPGS and HSA suitable candidates as carriers for valrubicin.

As expected, reduction enhanced the valrubicin carrying capacity of HSA. This increase in valrubicin solubility is probably due to the partial unfolding of HSA molecules following the breakage of disulfide bonds. In a reduced HSA characterization experiment, the blue shift and lower fluorescence intensity was also noted by Lee et al. as a fluorescence emission signature of HSA partial reduction, a transitional state in which HSA globule becomes molten, less compact, but can still revert back to its native structure when reintroduced to renaturing conditions (Young Lee & Hirose, 1992). The molten globule-like state can explain the translucent appearance of the rHSA only solution (Fig 21B). In that state, the additional free sulfhydryl groups can engage in intermolecular interaction, and more valrubicin molecules can be trapped in between the self - assembled molecules.

The self-assembled HSA structure is evidenced by the increase in the particle diameter size through DLS as compared to a suspension made of normal HSA and valrubicin (Table 5).The zeta potential value of rHSA-valrubicin complex suggests the suspension is composed of relatively stable particles (Bhattacharjee, 2016) although for a colloidal suspension such as rHSA-valrubicin, more extensive stability studies are needed. The corona distinctly seen on the TEM is probably made of layer of HSA molecule network adsorbing onto the surface of the self-assembled HSA structure, a phenomenon often reported when nanoparticles are in a biological surroundings (Kokkinopoulou, Simon, Landfester, Mailänder, & Lieberwirth, 2017). Thus, perhaps, not all HSA molecules were involved in the formation of self-assembled HSA complexes. A PDI value less than 0.2 is desirable for a nanoparticle preparation with biomedical applications and suggests uniformity of the preparation. The relatively high PDI value of the rHSA-valrubicin (Table 5) prepared as previously described suggested a heterogeneity in the nanoparticle population. This heterogeneity is confirmed on the TEM images which shows the presence HSA molecule assemblies of varied sizes (Fig.22).

The increase in percent cell viability both in HIO180 cells and HeyA8 cells- although inconsistent in the latter- upon treatment of rHSA alone can be attributed to the use the rHSA as an additional nutrient source. However, the high IC_{50} of rHSA-valrubicin compared to the free valrubicin suggests a protective effect of the rHSA on HIO180 cells. In contrast, the malignant HeyA8 cells were more sensitive the rHSA-valrubicin treatment. A possible explanation is that that the malignant HeyA8 cells have alternate cellular mechanisms that is either weakly active or not present in the HIO180 cells as it is often the case with malignant phenomena. For example, macropinocytosis is a process by which eukaryotic cells engulf some of the extracellular fluid, and several studies have shown that this endocytic pathway is frequently induced in cancer,

especially in Ras-transformed cells as a metabolic adaptation for nutrient scavenging (Commisso et al., 2013; Recouvreux & Commisso, 2017). Macropinocytosis is also a major route by which HSA is internalized by tumor cells (Stehle et al., 1997). Although HeyA8 cells are not Ras - transformed cells, it is possible they take in rHSA-valrubicin more readily than normal cells and thus accumulate higher levels of valrubicin intracellularly. The slow release profile of rHSA-valrubicin suggests that the rHSA-valrubicin could be used for targeted delivery as a high percentage of valrubicin can be retained in the self-assembling HSA molecules.

With TPGS, the increasing anisotropy observed with increasing TPGS concentration suggests valrubicin is indeed associated with a larger structure (micelle), and the increasing fluorescence intensity past the CMC of TPGS suggests that valrubicin is shielded from the external environment. The quenching occurring before the CMC is reached is probably due to the increased random collision of valrubicin molecules with molecules in their surrounding including individual TPGS molecules since micelles have not started forming yet. Taken together, anisotropy and the change in fluorescence intensity confirm that valrubicin is loaded in TPGS micelles (Fig. 33). The CMC (47 μg/mL) is lower than the usual CMC (200 μg/mL) reported in the literature at 37^{o}C. , Sadoqi et al also reported a CMC of 20 μM for TPGS for conditions similar to those used in this study and mentioned the temperature difference and methods of assessments such as measuring conductivity or change in surface tension instead of fluorometric measurements as factors for the discrepancy in the CMC values (Sadoqi, Lau-Cam, & Wu, 2009).

The TEM images on TPGS-valrubicin corroborated the DLS measurement values which suggested small particle diameter and high homogeneity. These results are consistent with the studies performed using TPGS only as drug carrier. For example, in their micellar preparation,

Muthu and colleagues reported a mean diameter size of 14 nm and mean PDI of 0.166 after mixing 0.1 mg coumarin 6 (a hydrophobic drug with anticancer properties) with 100 mg TPGS using a solvent casting method as well (Muthu et al., 2012). Although the zeta potential of the TPGS-valrubicin preparation was found to be low (Table 7) and suggested an unstable formulation, the slow release of the valrubicin observed in the *in vitro* drug release study showed that the TPGS-valrubicin micelles were stable under these conditions for 96 hours. During cytotoxicity studies, HeyA8 cells were more sensitive to TPGS than free valrubicin whereas HIO180 cells did not benefit from any significant protective effect from TPGS in the TPGS-valrubicin formulation. This may be explained by the fact that TPGS can readily enters cells indiscriminately through diffusion due to the small size of TPGS micelles (Traber, 1987). Thus, grafting a targeting moiety onto the surface of the valrubicin-loaded TPGS micelles would be key in not only avoiding off-target effects, but also in increasing the size of the particle enough to avoid renal clearance.

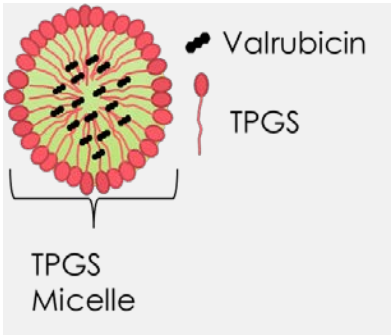

Figure 33: Pictorial Illustration of a Valrubicin-Loaded TPGS Micelle.

The larger diameter size of rHSA-valrubicin compared to the TPGS micelles loaded with valrubicin was to be expected since HSA already has a much higher molecular weight than TPGS. However, the low homogeneity of the rHSA-valrubicin warrants a revision of the method

of preparation. Although this study has shown the enhancing effect of rHSA on valrubicin solubility, a preparation method can be developed as to increase uniformity in rHSA- valrubicin suspension. Involving microfluidic mixing system in the preparation for a controlled production of the suspension may optimize the diameter size and PDI of the preparation. Also, in the field of nanoformulations, various techniques are used to fabricate albumin-bound drugs. Conventional techniques involve desolvation, thermal gelation, self -assembly, emulsification and nanospray drying (Fig. 34).

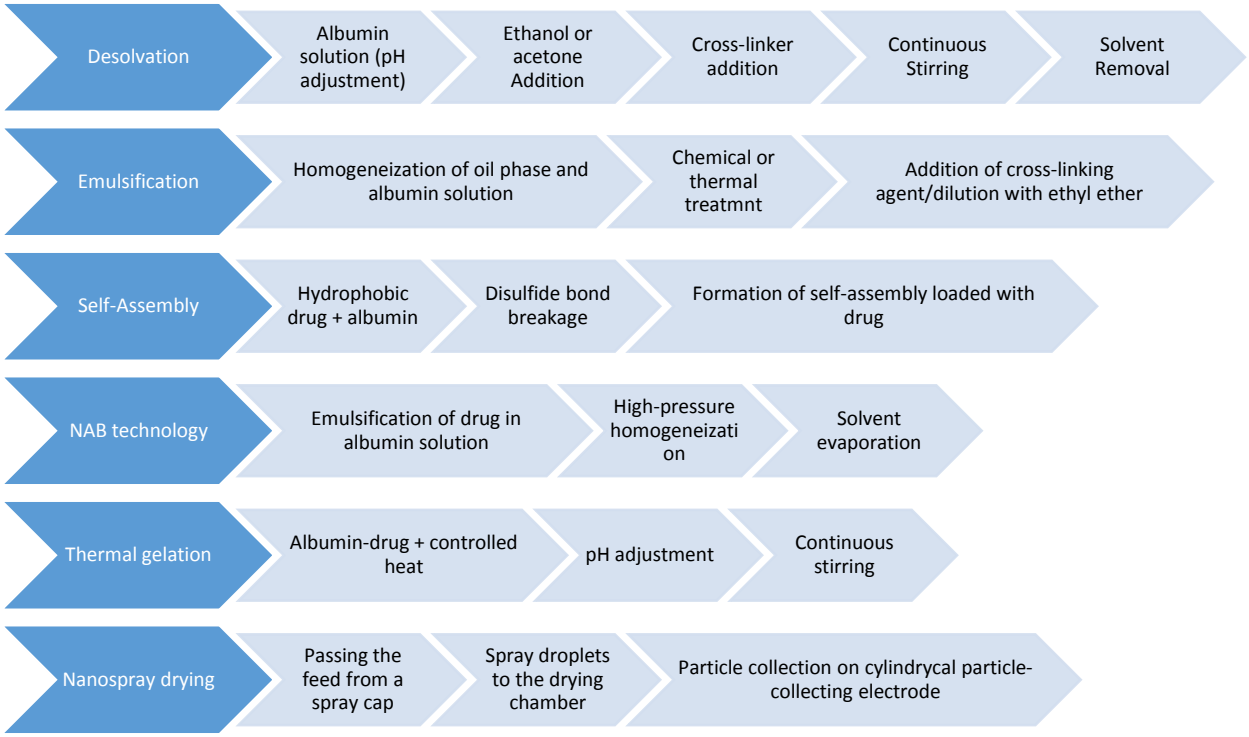

Figure 34: Fabrication Methods for Albumin-Bound Drugs (adapted from Kouchakzadeh, 2015). Chemical-based techniques involve desolvation, emulsification and self-assembly. Physical-based techniques use heat or pressure and include NAB technology, thermal gelation and nanospray drying.

In this study, the self- assembly method was chosen since it works best for hydrophobic drugs such as valrubicin and involves less chemical variables in the process (Kouchakzadeh, Safavi, & Shojaosadati, 2015). It would be interesting to investigate the combination of using the high-pressure homogenization in the nanoparticle albumin-bound (NAB) technology and self-assembly in preparing rHSA-valrubicin since NAB technology works for hydrophobic drugs as well.

In future studies, cellular uptake studies will help confirm the selective accumulation of valrubicin in HeyA8 cells versus HIO180 cells in the case of rHSA-valrubicin. These studies will provide insight as to the effective intracellular delivery of valrubicin by the TPGS micelles. Long term and relatively short-term stability studies under different storage conditions will need to be performed both on the rHSA-valrubicin and TPGS-valrubicin formulations. Fast protein liquid chromatography (FPLC) is an efficient purification method of a mixture protein, and in this case, it will be used to further characterize the rHSA-valrubicin in two aspects. First, using an adequate size exclusion column on the FPLC, the rHSA-valrubicin assemblies can be separated by their total molecular size which will serve the purification purpose. Second, each of these rHSA-valrubicin assemblies can then be characterized and compared in term of drug delivery efficiency. FPLC can also be applied to TPGS-valrubicin to estimate the number of TPGS forming a micelle and the number of valrubicin molecules contained in the micelle.

REFERENCES

Aarons, L., Grennan, D. M., & Siddiqui, M. (1983). The binding of ibuprofen to plasma proteins. *European Journal of Clinical Pharmacology*, *25*(6), 815–818.

American Cancer Society (2016). *Cancer Treatment & Survivorship: Facts & Figures*. *American Cancer Society*. Atlanta. Retrieved from https://www.cancer.org/content/dam/cancer-org/research/cancer-facts-and-statistics/cancer-treatment-and-survivorship-facts-and-figures/cancer-treatment-and-survivorship-facts-and-figures-2016-2017.pdf

Bachur, N. R. (1989). Anthracycline Antibiotics BT - Cancer Management in Man: Biological Response Modifiers, Chemotherapy, Antibiotics, Hyperthermia, Supporting Measures. In P. V Woolley (Ed.) (pp. 125–130). Dordrecht: Springer Netherlands.

Baudino, T. (2015). Targeted Cancer Therapy: The Next Generation of Cancer Treatment. *Current Drug Discovery Technologies*, *12*(1), 3–20.

Bhattacharjee, S. (2016). DLS and zeta potential - What they are and what they are not? *Journal of Controlled Release*, *235*, 337–351.

Bhushan, B., Khanadeev, V., Khlebtsov, B., Khlebtsov, N., & Gopinath, P. (2017). Impact of albumin based approaches in nanomedicine: Imaging, targeting and drug delivery. *Advances in Colloid and Interface Science*, *246*(July), 13–39.

Campos, F. C., Victorino, V. J., Martins-Pinge, M. C., Cecchini, A. L., Panis, C., & Cecchini, R.

(2014). Systemic toxicity induced by paclitaxel in vivo is associated with the solvent cremophor EL through oxidative stress-driven mechanisms. *Food and Chemical Toxicology*, *68*, 78–86.

Chatterjee, M., Ben-Josef, E., Robb, R., Vedaie, M., Seum, S., Thirumoorthy, K., … Williams, T. M. (2017). Caveolae-mediated endocytosis is critical for albumin cellular uptake and response to albumin-bound chemotherapy. *Cancer Research*, *77*(21), 5925–5937.

Chen, F., Wu, J., Zheng, C., Zhu, J., Zhang, Y., You, X., … Ge, L. (2016). TPGS modified reduced bovine serum albumin nanoparticles as a lipophilic anticancer drug carrier for overcoming multidrug resistance. *J. Mater. Chem. B*, *4*(22), 3959–3968.

Chen, J., Wang, M., Xi, B., Xue, J., He, D., Zhang, J., & Zhao, Y. (2012). SPARC is a key regulator of proliferation, apoptosis and invasion in human ovarian cancer. *PLoS ONE*, *7*(8), 1–15.

Commisso, C., Davidson, S. M., Soydaner-Azeloglu, R. G., Parker, S. J., Kamphorst, J. J., Hackett, S., … Bar-Sagi, D. (2013). Macropinocytosis of protein is an amino acid supply route in Ras-transformed cells. *Nature*, *497*(7451), 633–637.

Danhier, F. (2016). To exploit the tumor microenvironment: Since the EPR effect fails in the clinic, what is the future of nanomedicine? *Journal of Controlled Release*, *244*, 108–121.

Desai, N., Trieu, V., Damascelli, B., & Soon-shiong, P. (2009). SPARC Expression Correlates with Tumor Response to Albumin-Bound Paclitaxel in Head and Neck Cancer Patients. *Translational Oncology*, *2*(2), 59–64.

Duhem, N., Danhier, F., & Préat, V. (2014). Vitamin E-based nanomedicines for anti-cancer drug delivery. *Journal of Controlled Release*, *182*, 33–44.

Elzoghby, A. O., Samy, W. M., & Elgindy, N. A. (2012). Albumin-based nanoparticles as potential controlled release drug delivery systems. *Journal of Controlled Release*, *157*(2), 168–182.

Endo Pharmaceuticals. (2011).VALSTAR®: Reference ID: 3038561. Retrieved from https://www.accessdata.fda.gov/drugsatfda_docs/label/2011/020892s013lbl.pdf

Evans, T. W. (2002). Review article: albumin as a drug--biological effects of albumin unrelated to oncotic pressure. *Alimentary Pharmacology & Therapeutics*, *16 Suppl 5*, 6–11.

Fan, Z., Chen, C., Pang, X., Yu, Z., Qi, Y., Chen, X., … Sha, X. (2015). Adding vitamin E-TPGS to the formulation of genexol-pm: Specially mixed micelles improve drug-loading ability and cytotoxicity against multidrug-resistant tumors significantly. *PLoS ONE*, *10*(4), 1–17.

Ganapathi, R., & Israel, M. (1981). Comparative effects of adriamycin and n-trifluoroacetyladriamycin-14-valerate on cell kinetics, chromosomal damage, and macromolecular synthesis in vitro. *Cancer Research*, *41*(7), 2745–2750.

Gnapareddy, B., Reddy Dugasani, S., Ha, T., Paulson, B., Hwang, T., Kim, T., … Park, S. H. (2015). Chemical and Physical Characteristics of Doxorubicin Hydrochloride Drug-Doped Salmon DNA Thin Films. *Scientific Reports*, *5*(July), 1–9.

Guo, Y., Luo, J., Tan, S., Otieno, B. O., & Zhang, Z. (2013). The applications of Vitamin E TPGS in drug delivery. *European Journal of Pharmaceutical Sciences.*

Hasanuddin, H. A. B., Affandi, M. M., Salama, M., & Tripathy, M. (2014). Micellization of D-α-tocopheryl polyethylene glycol 1000 succinate (TGPS 1000): Thermodynamics and

related solute solvent interactions. *Oriental Journal of Chemistry*, *30*(3), 1119–1123.

Hauge, E., Christiansen, H., Rosada, C., De Darkó, E., Dam, T. N., & Stenderup, K. (2012). Topical valrubicin application reduces skin inflammation in murine models. *British Journal of Dermatology*, *167*(2), 288–295.

Israel, M., Idriss, J., Koseki, Y., & Khetarpal, V. (1987). Comparative effects of adriamycin and DNA-non-binding analogues on DNA, RNA, and protein synthesis in vitro. *Cancer Chemotherapy and Pharmacology*, *20*(4), 277–284.

Israel, M., Modest, E. J., & Frei, E. (1975). N-Trifluoroacetyladriamycin-14-valerate, an Analog with Greater Experimental Antitumor Activity and Less Toxicity than Adriamycin. *Cancer Research*, *35*(5), 1365–1368.

Kokkinopoulou, M., Simon, J., Landfester, K., Mailänder, V., & Lieberwirth, I. (2017). Visualization of the protein corona: towards a biomolecular understanding of nanoparticle-cell-interactions, 8858–8870.

Kouchakzadeh, H., Safavi, M. S., & Shojaosadati, S. A. (2015). Efficient Delivery of Therapeutic Agents by Using Targeted Albumin Nanoparticles. *Advances in Protein Chemistry and Structural Biology* (1st ed., Vol. 98). Elsevier Inc.

Kratz, F. (2008). Albumin as a drug carrier: Design of prodrugs, drug conjugates and nanoparticles. *Journal of Controlled Release*, *132*(3), 171–183.

Kratz, F. (2014). A clinical update of using albumin as a drug vehicle-A commentary. *Journal of Controlled Release*, *190*, 331–336.

Kudarha, R. R., & Sawant, K. K. (2017). Albumin based versatile multifunctional nanocarriers

for cancer therapy: Fabrication, surface modification, multimodal therapeutics and imaging approaches. *Materials Science and Engineering C*, *81*(July), 607–626.

Larsen, M. T., Kuhlmann, M., Hvam, M. L., & Howard, K. A. (2016). Albumin-based drug delivery: harnessing nature to cure disease. *Molecular and Cellular Therapies*, *4*(1), 3.

Li, Y., Hong, J., Li, H., Qi, X., Guo, Y., Han, M., & Wang, X. (2017). Genkwanin nanosuspensions: a novel and potential antitumor drug in breast carcinoma therapy. *Drug Delivery*, *24*(1), 1491–1500.

Maeda, H., Wu, J., Sawa, T., Matsumura, Y., & Hori, K. (2000). Tumor vascular permeability and the EPR effect in macromolecular therapeutics : a review. *Journal of Controlled Release*, *65*, 271–284.

Markman, M., Homesley, H., Norberts, D. A., Schink, J., Abbas, F., Miller, A., … Sweatman, T. (1996). Phase 1 trial of intraperitoneal AD-32 in gynecologic malignancies. *Gynecologic Oncology*, *61*(1), 90–93.

Maruthamuthu, M., & Kishore, S. (1987). Binding of naproxen to bovine serum albumin and tryptophan-modified bovine serum albumin. *Proceedings of the Indian Academy of Sciences - Chemical Sciences*, *99*(4), 273–279.

McGowan, J. V., Chung, R., Maulik, A., Piotrowska, I., Walker, J. M., & Yellon, D. M. (2017). Anthracycline Chemotherapy and Cardiotoxicity. *Cardiovascular Drugs and Therapy*, *31*(1), 63–75.

Merlot, A. M., Kalinowski, D. S., & Richardson, D. R. (2014). Unraveling the mysteries of serum albumin-more than just a serum protein. *Frontiers in Physiology*, *5* (August), 1–7.

Miele, E., Spinelli, G. P., Miele, E., Tomao, F., & Tomao, S. (2009). Albumin-bound formulation of paclitaxel (Abraxane ® ABI-007) in the treatment of breast cancer. *International Journal of Nan*, *4*, 99–105.

Muthu, M. S., Avinash Kulkarni, S., Liu, Y., & Feng, S.-S. (2012). Development of docetaxel-loaded vitamin E TPGS micelles: formulation optimization, effects on brain cancer cells and biodistribution in rats. *Nanomedicine*, *7*(3), 353–364.

National Cancer Institute (2015). What is cancer? Retrieved from https://www.cancer.gov/about-cancer/understanding/what-is-cancer

Narvekar, M., Xue, H. Y., Eoh, J. Y., & Wong, H. L. (2014). Nanocarrier for Poorly Water-Soluble Anticancer Drugs—Barriers of Translation and Solutions. *AAPS PharmSciTech*, *15*(4), 822–833.

Neophytou, C. M., Constantinou, C., Papageorgis, P., & Constantinou, A. I. (2014). D-alpha-tocopheryl polyethylene glycol succinate (TPGS) induces cell cycle arrest and apoptosis selectively in Survivin-overexpressing breast cancer cells. *Biochemical Pharmacology*, *89*(1), 31–42.

Onrust, S. V, & Lamb, H. M. (1999). Valrubicin. *Drugs & Aging*, *15*(1), 69–75.

Petitpas, I., Bhattacharya, A. A., Twine, S., East, M., & Curry, S. (2001). Crystal Structure Analysis of Warfarin Binding to Human Serum, *276*(25), 22804–22809.

PMC isochem. (2018). *Vitamin E TPGS NF * and Food Grade NF and Food Grade*. Vert-Le - Petit France. Retrieved from https://pmcisochem.fr/sites/default/files/documents/ISOCHEM TPGS 2015 08.pdf

Potmesil, M., Silber, R., Israel, M., Goldfeder, A., & Khetarpal, V. K. (1981). Protein-associated DNA Breaks and DNA-Protein Cross-Links Caused by DNA Nonbinding Derivatives of Adriamycin in L1210 Cells. *Cancer Research*, *41*(3), 1006–1010.

PubChem (2018). Doxorubicin. Retrieved from https://pubchem.ncbi.nlm.nih.gov/compound/doxorubicin#section=Top

PubChem (2018). Valrubicin. Retrieved from https://pubchem.ncbi.nlm.nih.gov/compound/Valrubicin

Recouvreux, M. V., & Commisso, C. (2017). Macropinocytosis : A Metabolic Adaptation to nutrient Stress in Cancer, *8*(September), 1–7.

Rizvi, S. F. A., Tariq, S., & Mehdi, M. (2018). Anthracyclines : Mechanism of Action , Classification , Pharmacokinetics and Future – A Mini Review. *International Journal of Biotechnology and Bioengineering*, *4*(4), 81–85.

Rosada, C., Stenderup, K., De Darkó, E., Dagnaes-Hansen, F., Kamp, S., & Dam, T. N. (2010). Valrubicin in a topical formulation treats psoriasis in a xenograft transplantation model. *Journal of Investigative Dermatology*, *130*(2), 455–463.

Sadoqi, M., Lau-Cam, C. A., & Wu, S. H. (2009). Investigation of the micellar properties of the tocopheryl polyethylene glycol succinate surfactants TPGS 400 and TPGS 1000 by steady state fluorometry. *Journal of Colloid and Interface Science*, *333*(2), 585–589.

Savla, R., Browne, J., Plassat, V., Wasan, K. M., & Wasan, E. K. (2017). Review and analysis of FDA approved drugs using lipid-based formulations. *Drug Development and Industrial Pharmacy*, *43*(11), 1743–1758.

Shah, A. R., & Banerjee, R. (2011). Colloids and Surfaces B : Biointerfaces Effect of d - ␣ - tocopheryl polyethylene glycol 1000 succinate (TPGS) on surfactant monolayers. *Colloids and Surfaces B: Biointerfaces*, *85*(2), 116–124.

Shah, S., Chib, R., Raut, S., Bermudez, J., Sabnis, N., Duggal, D., … Gryczynski, I. (2016). Photophysical characterization of anticancer drug valrubicin in rHDL nanoparticles and its use as an imaging agent. *Journal of Photochemistry and Photobiology. B, Biology*, *155*, 60–65.

Sleep, D., Cameron, J., & Evans, L. R. (2013). Albumin as a versatile platform for drug half-life extension. *Biochimica et Biophysica Acta (BBA) - General Subjects*, *1830*(12), 5526–5534.

Stehle, G., Sinn, H., Wunder, A., Hermann, H., Stewart, J. C. M., Hartung, G., … Ludwig, D. (1997). Oncology Plasma protein (albumin) catabolism by the tumor itself-implications for tumor metabolism and the genesis of cachexia, *8428*(97).

Štěrba, M., Popelová, O., Vávrová, A., Jirkovský, E., Kovaříková, P., Geršl, V., & Šimůnek, T. (2013). Oxidative Stress, Redox Signaling, and Metal Chelation in Anthracycline Cardiotoxicity and Pharmacological Cardioprotection. *Antioxidants & Redox Signaling*, *18*(8), 899–929.

Strickley, R. G. (2004). Solubilizing Excipients in Oral and Injectable Formulations. *Pharmaceutical Research*, *21*(2), 201–230.

Szebeni, J., Muggia, F. M., & Alving, C. R. (1998). Complement activation by Cremophor EL as a possible contributor to hypersensitivity to paclitaxel: An in vitro study. *Journal of the National Cancer Institute*, *90*(4), 300–306.

Traber, G. (1987). Uptake of intact TPGS (d-a-tocopheryl a water-miscible form by human cells in vitro13 polyethylene of vitamin.

Tran, S., Degiovanni, P. J., Piel, B., & Rai, P. (2017). Cancer nanomedicine : a review of recent success in drug delivery. *Clinical and Translational Medicine*, 6:44.

Vecchi, A., Spreafico, F., Sironi, M., Cairo, M., & Garattini, S. (1980). The immunodepressive and hematotoxic activities of N-trifluoro-acetyl-adriamycin-14-valerate. *European Journal of Cancer (1965)*, *16*(10), 1289–1296.

Wagner, B. A., Buettner, G. R., & Burns, C. P. (1996). Vitamin E slows the rate of free radical-mediated lipid peroxidation in cells. *Archives of Biochemistry and Biophysics*, *334*(2), 261–267.

Wang, W., Huang, Y., Zhao, S., Shao, T., & Cheng, Y. (2013). Human serum albumin (HSA) nanoparticles stabilized with intermolecular disulfide bonds. *Chem. Commun.*, *49*(22), 2234–2236.

Weiss, R. B., Donehower, R. C., Wiernik, P. H., Ohnuma, T., Gralla, R. J., Trump, D. L., … Leyland-Jones, B. (1990). Hypersensitivity reactions from taxol. *Journal of Clinical Oncology*, *8*(7), 1263–1268.

WHO (2018). *Cancer*. Retrieved from http://www.who.int/cancer/en

Yan, A., Von Dem Bussche, A., Kane, A. B., & Hurt, R. H. (2007). Tocopheryl Polyethylene Glycol Succinate as a Safe, Antioxidant Surfactant for Processing Carbon Nanotubes and Fullerenes. *Carbon*, *45*(13), 2463–2470.

Yang, C., Wu, T., Qi, Y., & Zhang, Z. (2018). Recent advances in the application of vitamin E

TPGS for drug delivery. *Theranostics*, *8*(2), 464–485.

Yardley, D. A. (2013). Nab-Paclitaxel mechanisms of action and delivery. *Journal of Controlled Release*, *170*(3), 365–372.

Young Lee, J., & Hirose, M. (1992). Partially Folded State of the Disulfide-reduced Form of Human Serum Albumin as an Intermediate for Reversible Denaturation *. *The Journal of Biological Chemistry*, *267*(21), 14753–14758.

Zhang, Y., Sun, T., & Jiang, C. (2018). Biomacromolecules as carriers in drug delivery and tissue engineering. *Acta Pharmaceutica Sinica B*, *8*(1), 34–50.

Zhang, Z., Tan, S., & Feng, S.-S. (2012). Vitamin E TPGS as a molecular biomaterial for drug delivery. *Biomaterials*, *33*(19), 4889–4906.

Zhao, L., & Zhang, B. (2017). Doxorubicin induces cardiotoxicity through upregulation of death receptors mediated apoptosis in cardiomyocytes. *Scientific Reports*, *7*(February), 1–11.